

DELAMINATION-FRETTING WEAR FAILURE  
EVALUATION AT HAP-TI-6AL-4V INTERFACE OF  
ARTIFICIAL HIP IMPLANT



PTTA UTHM  
PERPUSTAKAAN TUNKU PUN AMINAH

UNIVERSITI TUN HUSSEIN ONN MALAYSIA

UNIVERSITI TUN HUSSEIN ONN MALAYSIA

STATUS CONFIRMATION FOR THESIS  
DOCTOR OF PHILOSOPHY

DELAMINATION-FRETTING WEAR FAILURE EVALUATION AT HAP-TI-6AL-4V  
INTERFACE OF ARTIFICIAL HIP IMPLANT

ACADEMIC SESSION: 2020/2021

I, **NAGENTRAU MUNIANDY**, agree to allow Thesis to be kept at the Library under the following terms:

1. This Thesis is the property of the Universiti Tun Hussein Onn Malaysia.
2. The library has the right to make copies for educational purposes only.
3. The library is allowed to make copies of this Thesis for educational exchange between higher educational institutions.
4. The library is allowed to make available full text access of the digital copy via the internet by Universiti Tun Hussein Onn Malaysia in downloadable format provided that the Thesis is not subject to an embargo. Should an embargo be in place, the digital copy will only be made available as set out above once the embargo has expired.
5. \*\* Please Mark (v)

CONFIDENTIAL

(Contains information of high security or of great importance to Malaysia as STIPULATED under the OFFICIAL SECRET ACT 1972) *Title and Abstract only*

RESTRICTED

(Contains restricted information as determined by the organization/institution where research was conducted)-  
*Title, Abstract and Introduction only*

EMBARGO

\_\_\_\_\_ until \_\_\_\_\_  
(date) (date)

FREE ACCESS

Approved by,

(WRITER'S SIGNATURE)

(SUPERVISOR'S SIGNATURE)

Permanent Address:

NO.6, LOT 875, PAYA  
BESAR, 09600 LUNAS,  
KEDAH

Date : \_\_\_\_\_

Date: \_\_\_\_\_

NOTE:

\*\* If this Thesis is classified as CONFIDENTIAL or RESTRICTED, please attach the letter from the relevant authority/organization stating reasons and duration for such classification.

This thesis has been examined on date 09<sup>th</sup> December 2020  
and is sufficient in fulfilling the scope and quality for the purpose of awarding the  
Degree of Doctor of Philosophy

Chairperson:

ASSOCIATE PROFESSOR TS. DR. AMIR BIN KHALID

Faculty of Engineering Technology

Universiti Tun Hussein Onn Malaysia

Assistant Chairperson:

TS. DR. NORAINI BINTI MARSI

Faculty of Engineering Technology

Universiti Tun Hussein Onn Malaysia

Examiners

PROF. DATO' DR. AHMAD MUJAHID BIN AHMAD ZAIDI

Faculty of Engineering

Universiti Pertahanan Nasional Malaysia

ASSOC. PROF. IR. TS. DR. AL EMRAN BIN ISMAIL

Faculty of Mechanical and Manufacturing Engineering

Universiti Tun Hussein Onn Malaysia



PTT A UTHM  
PERPUSTAKAAN TUNKU TUN AMINAH

DELAMINATION-FRETTING WEAR FAILURE EVALUATION AT HAP-TI-  
6AL-4V INTERFACE OF ARTIFICIAL HIP IMPLANT

NAGENTRAU S/O MUNIANDY

A thesis submitted in  
fulfilment of the requirement for the award of the  
Doctor of Philosophy



PTTAUTHM  
PERPUSTAKAAN TUNKU TUN AMINAH

Faculty of Engineering Technology  
Universiti Tun Hussein Onn Malaysia

MARCH 2021

I hereby declare that the work in this project report is my own except for quotations  
and summaries which have been duly acknowledged

Student : .....

NAGENTRAU MUNIANDY

Date : .....

Supervisor : .....

ASSOC. PROF. TS. DR. SAIFULNIZAN JAMIAN



PTTAUTHM  
PERPUSTAKAAN TUNKU TUN AMINAH

***“IT’S NOT THE LOAD THAT BREAKS YOU DOWN, IT’S THE WAY  
YOU CARRY IT”***

**To my beloved mother and father,**

Mr. Muniandy & Mdm. Nookkaretnam

*For being the backbone of my life by supporting me from the very beginning*

**To my supervisor and mentors,**

Assoc. Prof. Ts. Dr. Saifulnizan Jamian

Dr. Abdul Latif Mohd. Tobi

Prof. Dr. Yuichi Otsuka

Ts. Dr. Rosniza Binti Hussin@Isa

*For their consistent encouragement, guidance and support throughout the  
research journey*

**To my siblings, family and friends**

Ms. Kumari Achana

Ms. Shangkari Muniandy

Mr. Prathabrao Muniandy

Close family members & true friends

*For their trust, cooperation and motivation during this project*

**To supporting company/organisation**

UOW Malaysia KDU University College

iCEE international Sdn. Bhd.

SHM Future Resources

*For their direct and indirect support in completing various stages of this  
research*



PTTA UTHM  
PERPUSTAKAAN TUN AMINAH

## ACKNOWLEDGEMENT

First and foremost, I praise the almighty God for blessing me strength and capability to complete my doctorate research successfully. This thesis dissertation owes its presence to the inspiration, encouragement and assistance from several good souls. My sincere gratitude is extended to my parents, siblings, close family members and friends for their unconditional and genuine love through my thick and thin.

My greatest appreciation goes to my supervisor, Dr. Abdul Latif Bin Mohd Tobi who has been constant source of guidance and motivational factor to take up this PhD challenge. I would like to express my deepest appreciation to my present supervisor, Assoc. Prof. Ts. Dr. Saifulnizan Bin Jamian for his consistent encouragement, flexible discussion time and most importantly his trust on me which boosted my effort in completing this research. I greatly appreciate Ts. Dr. Rosniza Binti Hussin@Isa, Ts. Dr. Nurasyikin Binti Misdan, Dr. Aimi Syamimi Binti Ab Ghafar and Ts. Dr. Azrin Hani Binti Abdul Rashid for their assistance and support from Faculty of Engineering Technology (FTK). A special appreciation goes to my mentor Ir. Dr. Thirumalaichelvam for keep inspiring me to achieve more. I am indebted to Prof. Dr. Yuichi Otsuka from Nagaoka University of Technology (NUT), Japan whose deepest knowledge in biomechanics field enhanced present work's quality.

I am grateful for financial assistance from The Ministry of Education Malaysia and Faculty of Engineering Technology (FTK), Universiti Tun Hussein Onn Malaysia (UTHM) during my research years. In addition, I am indebted to supportive companies/organisations such as UOW Malaysia KDU University College, iCEE international Sdn. Bhd. and SHM Future Resources for their unflinching support and unconditional love throughout my doctorate journey. I would never forget all the good-hearted personalities that have been an indispensable impetus who contributed directly nor indirectly throughout this research. Last but not least, I wholeheartedly dedicate this thesis dissertation to individuals who constantly striving for excellence in life.



## ABSTRACT

Osteoarthritis due to rapid aging population in Malaysia and developed countries leads to an extensive application of titanium artificial hip implants. However, titanium alloys (Ti-6Al-4V) cannot directly adhere with human bone due to bio-compatibility issue. Thus, Hydroxyapatite (HAp:Ca<sub>10</sub>(PO<sub>4</sub>)(OH)<sub>2</sub>) coating which consists of main composition of human bone is plasma sprayed on titanium implants to maintain fixations during bone in-growth process. HAp coatings are susceptible to fail due to brittle fractures (coating through thickness crack) to initiate delamination which promotes fretting wear behaviour. Fretting wear particles are concerned for activating inflammations at surrounding organs, which lead to loosening of implants or subsequent failures. Present research aims to develop a finite element model to examine delamination-fretting wear behaviours that can suitably mimic actual loading conditions at HAp-Ti-6Al-4V interface of hip implant femoral stem component to formulate maximum wear depth predictive equation as a novel and fast failure prediction tool. Three simple finite element contact configuration models subjected to different mechanical and tribological properties consist of contact pad (bone), HAp coating and Ti-6Al-4V substrate are developed using contact modelling, cohesive zone modelling (CZM) and adaptive wear modelling (UMESHMOTION) approaches to be examined under static simulation. The developed finite element models are validated and verified with modified Hertzian theoretical solution and reported literatures. The findings revealed that significant delamination-fretting wear is recorded at contact edge (leading edge) as a result of substantial contact pressure and contact slip driven by stress singularity effect. Tensile-compressive condition ( $R = -1$ ) experiences most significant delamination-fretting wear behaviour (8 times higher) compared to stress ratio  $R = 0.1$  and  $R = 10$ . Finally, maximum delamination-fretting wear depth predictive equations are successfully formulated with significant goodness of fit and reliability as a fast failure prediction tool.



## ABSTRAK

*Osteoarthritis* disebabkan populasi penuaan yang pantas di Malaysia dan negara maju yang lain membawa kepada penggunaan prostesis pinggul aloi titanium secara meluas. Namun, aloi titanium tidak dapat dicantum secara langsung pada tulang manusia disebabkan masalah ketakserasian bio. Oleh itu, lapisan Hidroksiapatit (HAp:Ca<sub>10</sub>(PO<sub>4</sub>)(OH)<sub>2</sub>) disalutkan pada prostesis pinggul untuk mengekalkan penetapan semasa proses pertumbuhan tulang. Lapisan HAp terdedah kepada keretakan ketebalan menyeluruh sampai antara muka HAp-Ti-6Al-4V dan menyebabkan delaminasi lapisan serta mempercepatkan proses haus penggeselsuaian. Partikel-partikel haus penggeselsuaian boleh mengaktifkan keradangan pada organ sekitarnya sehingga boleh melonggarkan prostesis pinggul serta kegagalan berikutnya. Penyelidikan ini bertujuan membangunkan model kaedah unsur terhingga (FEM) untuk menganalisis haus penggeselsuaian-delaminasi pada antara muka HAp-Ti-6Al-4V yang tertakluk kepada keadaan beban yang sebenar dan merumuskan persamaan ramalan kedalaman maksimum haus penggeselsuaian-delaminasi sebagai alat ramalan kegagalan yang pantas. Tiga model FEM yang terdiri daripada pad kontak, lapisan HAp dan substrat Ti-6Al-4V tertakluk kepada sifat mekanikal dan tribologikal yang berbeza dibangunkan menggunakan pendekatan *contact modelling*, *cohesive zone modelling (CZM)* dan *adaptive wear modelling (UMESHMOTION)* untuk dikaji di bawah simulasi statik. Model FEM disahkan dengan teori Hertzian yang diubahsuai dan kajian sebelumnya. Hasil kajian menunjukkan bahawa haus penggeselsuaian-delaminasi yang ketara direkodkan pada pinggir kontak disebabkan singulariti tegasan didorong oleh tekanan sentuh dan slip sentuh. Nisbah tegasan ( $R = -1$ ) menunjukkan haus penggeselsuaian-delaminasi yang 8 kali lebih tinggi berbanding dengan nisbah tegasan  $R = 0.1$  and  $R = 10$ . Akhirnya, persamaan ramalan kedalaman maksimum haus penggeselsuaian-delaminasi berjaya dirumuskan dengan ketepatan dan reliabiliti yang tinggi untuk digunakan sebagai alat ramalan kegagalan yang pantas dan tepat.

## CONTENTS

<b>TITLE</b>	<b>i</b>
<b>DECLARATION</b>	<b>ii</b>
<b>DEDICATION</b>	<b>iii</b>
<b>ACKNOWLEDGEMENT</b>	<b>iv</b>
<b>ABSTRACT</b>	<b>v</b>
<b>ABSTRAK</b>	<b>vi</b>
<b>CONTENTS</b>	<b>vii</b>
<b>LIST OF TABLES</b>	<b>xiv</b>
<b>LIST OF FIGURES</b>	<b>xv</b>
<b>LIST OF SYMBOLS AND ABBREVIATIONS</b>	<b>xxvi</b>
<b>LIST OF APPENDICES</b>	<b>xxix</b>
<b>CHAPTER 1 INTRODUCTION</b>	<b>1</b>
1.1 Background of study	1
1.2 Problem statement	4
1.3 Research questions	6
1.4 Research objectives	7
1.5 Research scopes and limitations	8
1.6 Research novelty	9
1.7 Research significance	9



1.8	Thesis organisation	10
<b>CHAPTER 2 LITERATURE REVIEW</b>		<b>12</b>
2.1	Introduction	12
2.2	Anatomy of hip joint	12
2.3	Hip joint disorders	14
2.4	Total hip replacement (THR) using artificial hip implant	15
2.5	Hydroxyapatite (HAp) coated uncemented THR	17
2.6	Material of artificial hip implant	18
2.7	Metallic artificial femoral stem	20
2.7.1	Stem material	22
2.7.2	Stem geometry	23
2.7.3	Stem surface finish	24
2.8	Principle of energy conservation and deforming materials	25
2.9	Contact mechanics	27
2.10	Fretting	33
2.11	Fretting fatigue in artificial femoral stem	35
2.12	HAp coating delamination	38
2.13	Fretting wear in artificial femoral stem	41
2.14	Delamination modelling	51
2.14.1	Cohesive zone modelling	51
2.14.2	Traction-separation law	52



2.15	Fretting wear modelling	56
2.15.1	Archard's wear law	58
2.15.2	Dissipated energy wear law	59
2.16	Summary and research gaps	60

## **CHAPTER 3 METHODOLOGY** **62**

3.1	Introduction	62
3.2	Research flow	62
3.3	Basic assumptions	64
3.4	Physical model	65
3.4.1	Specimen preparation	66
3.4.2	Contact pad preparation	67
3.4.3	Fretting fatigue experimental arrangement	68
3.5	Contact modelling: Stage-1	69
3.5.1	Part modelling	70
3.5.2	Part assembly	71
3.5.3	Material allocation	72
3.5.4	Model meshing	73
3.5.5	Mesh sensitivity analysis	74
3.5.6	Contact interaction	75
3.5.7	Boundary condition and step configuration	76
3.5.8	Assessment of parameters	79



3.5.9	Result analysis technique	81
3.5.10	Contact modelling validation	82
3.6	Cohesive zone modelling (CZM): Stage-2	84
3.6.1	Part modelling	86
3.6.2	Part assembly	87
3.6.3	Material allocation	88
3.6.4	Model meshing	90
3.6.5	Mesh sensitivity analysis	90
3.6.6	Contact interaction	91
3.6.7	Boundary condition and step configuration	92
3.6.8	Assessment parameter	93
3.6.9	Result analysis technique	94
3.6.10	Cohesive zone modelling verification and validation	95
3.7	Delamination-fretting wear modelling (Stage-3)	97
3.7.1	ABAQUS delamination-fretting wear modelling	99
3.7.2	Part modelling	100
3.7.3	Part assembly	101
3.7.4	Material allocation	101
3.7.5	Model meshing	102
3.7.6	Contact interaction	103



3.7.7	Boundary condition and step configuration	104
3.7.8	Delamination-fretting wear computational model	105
3.7.9	Arbitrary Lagrangian Eulerian (ALE) adaptive meshing	107
3.7.10	Assessment parameters	109
3.7.11	Result analysis	110
3.7.12	Cycle jump analysis	111
3.7.13	Delamination-fretting wear model validation and verification	112
3.8	Multiple linear regression model	113
3.9	Summary	114
<b>CHAPTER 4 RESULTS AND DISCUSSION</b>		<b>116</b>
4.1	Introduction	116
4.2	Contact pressure and contact slip analysis (Stage-1)	116
4.2.1	Effect of delamination length	117
4.2.2	Effect of loading condition	125
4.2.3	Effect of bone elastic modulus	134
4.2.4	Discussion	145
4.3	Interface damage and delamination initiation analysis (Stage-2)	153



4.3.1	Effect of loading condition	155
4.3.2	Effect of bone elastic modulus	160
4.3.3	Discussion	165
4.4	Cohesive element interfacial parameter analysis (Stage-2)	169
4.4.1	Effect of interface strength	170
4.4.2	Effect of interface stiffness	172
4.4.3	Effect of interface energy release rate	174
4.4.4	Discussion	176
4.5	Delamination-fretting wear analysis (Stage-3)	181
4.5.1	Effect of delamination length	182
4.5.2	Effect of loading condition under different stress ratio	184
4.5.3	Effect of bone elastic modulus	186
4.5.4	Effect of cycle number	188
4.5.5	Contact pressure and contact slip evolutions	190
4.5.6	Discussion	192
4.6	Formulating maximum delamination-fretting wear depth predictive equation	197
4.7	Validation of formulated predictive equation	204
4.8	Summary	205



<b>CHAPTER 5 CONCLUSION AND RECOMMENDATION</b>	<b>209</b>
5.1 Conclusion	209
5.2 Knowledge contribution	211
5.3 Recommendation for future works	213
<b>REFERENCES</b>	<b>215</b>
<b>LIST OF PUBLICATION</b>	<b>226</b>
<b>APPENDICES</b>	<b>227</b>
<b>VITA</b>	<b>251</b>



**PTTA UTHM**  
PERPUSTAKAAN TUNKU TUN AMINAH



**LIST OF TABLES**

3.1	Abaqus consistent unit	64
3.2	Contact modelling material data	73
3.3	Range of assigned mechanical and tribological parameters	81
3.4	Traction-separation law interfacial parameter	89
3.5	Cohesive zone modelling mechanical and tribological variables	94
3.6	Cohesive zone modelling interfacial variables	94
3.7	Delamination-fretting wear modelling mechanical and tribological variables	110



## LIST OF FIGURES

1.1	Hip joint anatomy	2
1.2	Osteoarthritis and total hip replacement (THR) surgery	2
1.3	Delamination-fretting wear failure mechanism	4
1.4	Possible delamination interface of HAp coated Ti-6Al-4V hip implant	6
2.1	Human hip joint anatomy	13
2.2	Osteoarthritis and total hip replacement (THR) surgery	15
2.3	Artificial hip implant parts	16
2.4	Uncemented and cemented total hip replacement (THR)	17
2.5	Typical procedures of HAp coated uncemented THR	18
2.6	Different artificial femoral stem designs	21
2.7	Different designs of artificial femoral stems	22
2.8	Load transfer patter with and without artificial hip implant	24
2.9	Human hip loading structure	27
2.10	Different types of contact	29
2.11	2D Hertzian contact schematic	30
2.12	Herztian equation of contact pressure distribution	31
2.13	Punch (flat) on flat contact configuration schematic	32
2.14	Rigid and frictionless punch indention on flat elastic space contact pressure distribution	32
2.15	Modes of fretting	34
2.16	Different fretting regime loops	34



2.17	Variables affecting fretting	35
2.18	Fretting fatigue of artificial hip implant	36
2.19	Fretting fatigue apparatus	37
2.20	SEM image of plasma sprayed HAp coated Ti-6Al-4V	38
2.21	Delamination behaviour in static and cyclic loading	39
2.22	SEM images of delamination at HAp-Ti-6Al-4V interface subjected to different cycle number (a) $N = 1.0 \times 10^3$ (b) $N = 1.0 \times 10^4$ and (c) $N = 1.0 \times 10^5$	40
2.23	Delamination comparison in SBF and normal condition	41
2.24	Different types of wear mechanism and fretting wear	43
2.25	Height profile changes at delamination tips subject to different loading condition (a) $R = -1$ , (b) $R = 10$ , (c) $R = 0.1$ and (d) static load	45
2.26	SEM image of wear debris under cyclic loading in normal condition (a) $R = -1$ , (b) $R = 10$ and (c) $R = 0.1$	46
2.27	SEM image of wear debris under cyclic loading in SBF (a) $R = -1$ , (b) $R = 10$ and (c) $R = 0.1$	47
2.28	SEM image of HAp coating wear behaviour (a) ejection of wear powders from tip of delamination and (b) embedding of wear powders in to pores in PP resin	48
2.29	Delamination length effect on wear behaviour (a) wear amounts at interface between HAp coating with Ti substrates and (b) wear amounts at interface between HAp coating with porous PP resins	49
2.30	Loading condition effect on wear behaviour (a) wear amounts at interface between HAp coating	



	with ti substrates and (b) wear amounts at interface between HAp coating with porous PP resins	50
2.31	Bilinear traction-separation interface constitutive relation	53
2.32	Finite element mesh and boundary condition	54
2.33	The SDEG contour plot of interfacial cohesive elements	55
2.34	Contact pressure distribution in hip joint implant FE model	58
2.35	The predicted wear depth and scar width validation	58
3.1	Overall research flowchart	63
3.2	Ti-6Al-4V specimen schematic diagram	66
3.3	HAp coating deposition on Ti-6Al-4V specimen	66
3.4	Contact pad preparation mould with HAp coated Ti-6Al-4V specimen	67
3.5	Contact pad bonded HAp coated Ti-6Al-4V specimen	67
3.6	Schematic illustration of fretting fatigue test arrangement	68
3.7	Fretting fatigue experimental test with in-situ observation	68
3.8	Stage-1 detailed flowchart: contact modelling	69
3.9	HAp coating with contact pad part as indenter	71
3.10	Ti-6Al-4V part as substrate	71
3.11	Complete assembly of contact pad, hap coating and Ti-6Al-4V	72
3.12	FE contact model mesh module	74
3.13	Mesh refinement at the contact region	74
3.14	Predicted maximum contact pressure variation with mesh size	75
3.15	Master and slave contact interaction	76
3.16	Contact property of HAp-Ti-6Al-4V interface	76
3.17	Model boundary condition	77
3.18	Contact interface tie constraint	77



3.19	FE model loading condition	78
3.20	History of contact simulation loading	79
3.21	Complete model to perform parametric study	80
3.22	Simulation result from odb file	82
3.23	Path line on Ti-6Al-4V substrate	82
3.24	Contact pressure distribution comparison between theoretical solution and FE simulation	84
3.25	Stage-2 detailed flowchart: cohesive zone modelling	85
3.26	Contact pad with HAp coating part	86
3.27	Ti-6Al-4V substrate part	87
3.28	Cohesive layer part	87
3.29	Complete assembly of cohesive zone modelling	88
3.30	Cohesive element layer position at interface	88
3.31	Cohesive zone modelling mesh module	90
3.32	Predicted delamination length variation with mesh size	91
3.33	Cohesive zone model contact interaction	92
3.34	Cohesive zone model boundary condition	93
3.35	Simulation result odb file of cohesive zone modelling analysis	95
3.36	Standard tension-delamination result comparison between experimental and FE simulation	96
3.37	Novel shear-delamination result comparison between experimental and FE simulation	96
3.38	Novel asymmetric four-point bending mixed-mode delamination result comparison between experimental and FE simulation	96
3.39	Cohesive zone model validation with experimental SEM image	97
3.40	Stage-3 detailed flowchart: delamination-fretting wear modelling	98
3.41	Linking ABAQUS/Standard with Intel Fortran compiler and Microsoft Visual Studio	100



3.42	Complete assembly of delamination-fretting wear model	101
3.43	Delamination-fretting model mesh	102
3.44	Delamination-fretting model contact interaction	103
3.45	Delamination-fretting model boundary condition	104
3.46	Delamination-fretting wear loading history	105
3.47	ALE nodes and adaptive mesh domain	108
3.48	Simulation result odb file of delamination-fretting wear model	110
3.49	Cycle jump effect on predicted delamination-fretting wear	111
3.50	SEM image of wear debris at delamination tips	112
3.51	Total wear at HAp-Ti-6Al-4V interface	113
4.1	Predicted contact pressure distribution under different delamination length for (a) normal loading, (b) maximum fatigue loading and (c) minimum fatigue loading ( $R = 0.1$ , $E_{bone} = 1 \text{ GPa}$ , $P_N = 20 \text{ MPa}$ , $\sigma_{fatigue} = 300 \text{ MPa}$ )	118
4.2	Predicted contact slip distribution under different delamination length for (a) normal loading, (b) maximum fatigue loading and (c) minimum fatigue loading ( $R = 0.1$ , $E_{bone} = 1 \text{ GPa}$ , $P_N = 20 \text{ MPa}$ , $\sigma_{fatigue} = 300 \text{ MPa}$ )	120
4.3	Predicted contact pressure distribution under different delamination length for (a) normal loading, (b) maximum fatigue loading and (c) minimum fatigue loading ( $R = 10$ , $E_{bone} = 1 \text{ GPa}$ , $P_N = 20 \text{ MPa}$ , $\sigma_{fatigue} = 300 \text{ MPa}$ )	121
4.4	Predicted contact slip distribution under different delamination length for (a) normal loading, (b) maximum fatigue loading and (c) minimum fatigue loading ( $R = 10$ , $E_{bone} = 1 \text{ GPa}$ , $P_N = 20 \text{ MPa}$ , $\sigma_{fatigue} = 300 \text{ MPa}$ )	122



- 4.5 Predicted contact pressure distribution under different delamination length for (a) normal loading, (b) maximum fatigue loading and (c) minimum fatigue loading ( $R = -1$ ,  $E_{bone} = 1 \text{ GPa}$ ,  $P_N = 20 \text{ MPa}$ ,  $\sigma_{fatigue} = 300 \text{ MPa}$ ) 124
- 4.6 Predicted contact slip distribution under different delamination length for (a) normal loading, (b) maximum fatigue loading and (c) minimum fatigue loading ( $R = -1$ ,  $E_{bone} = 1 \text{ GPa}$ ,  $P_N = 20 \text{ MPa}$ ,  $\sigma_{fatigue} = 300 \text{ MPa}$ ) 125
- 4.7 Predicted contact pressure distribution under different loading condition for (a) normal loading, (b) maximum fatigue loading and (c) minimum fatigue loading ( $R = 0.1$ ,  $E_{bone} = 1 \text{ GPa}$ ,  $Del = 1.0 \text{ mm}$ ) 127
- 4.8 Predicted contact slip distribution under different loading condition for (a) normal loading, (b) maximum fatigue loading and (c) minimum fatigue loading ( $R = 0.1$ ,  $E_{bone} = 1 \text{ GPa}$ ,  $Del = 1.0 \text{ mm}$ ) 128
- 4.9 Predicted contact pressure distribution under different loading condition for (a) normal loading, (b) maximum fatigue loading and (c) minimum fatigue loading ( $R = 10$ ,  $E_{bone} = 1 \text{ GPa}$ ,  $Del = 1.0 \text{ mm}$ ) 130
- 4.10 Predicted contact slip distribution under different loading condition for (a) normal loading, (b) maximum fatigue loading and (c) minimum fatigue loading ( $R = 10$ ,  $E_{bone} = 1 \text{ GPa}$ ,  $Del = 1.0 \text{ mm}$ ) 131
- 4.11 Predicted contact pressure distribution under different loading condition for (a) normal loading, (b) maximum fatigue loading and (c) minimum fatigue loading ( $R = -1$ ,  $E_{bone} = 1 \text{ GPa}$ ,  $Del = 1.0 \text{ mm}$ ) 132
- 4.12 Predicted contact slip distribution under different loading condition for (a) normal loading,



- (b) maximum fatigue loading and (c) minimum fatigue loading ( $R = -1$ ,  $E_{\text{bone}} = 1 \text{ GPa}$ ,  $\Delta l = 1.0 \text{ mm}$ ) 134
- 4.13 Predicted contact pressure distribution under different bone elastic modulus for (a) normal loading, (b) maximum fatigue loading and (c) minimum fatigue loading ( $R = 0.1$ ,  $P_N = 20 \text{ MPa}$ ,  $\sigma_{\text{fatigue}} = 300 \text{ MPa}$ ,  $\Delta l = 1.0 \text{ mm}$ ) 136
- 4.14 Predicted contact slip distribution under different bone elastic modulus for (a) normal loading, (b) maximum fatigue loading and (c) minimum fatigue loading ( $R = 0.1$ ,  $P_N = 20 \text{ MPa}$ ,  $\sigma_{\text{fatigue}} = 300 \text{ MPa}$ ,  $\Delta l = 1.0 \text{ mm}$ ) 137
- 4.15 Predicted contact pressure distribution under different bone elastic modulus for (a) normal loading, (b) maximum fatigue loading and (c) minimum fatigue loading ( $R = 10$ ,  $P_N = 20 \text{ MPa}$ ,  $\sigma_{\text{fatigue}} = 300 \text{ MPa}$ ,  $\Delta l = 1.0 \text{ mm}$ ) 139
- 4.16 Predicted contact slip distribution under different bone elastic modulus for (a) normal loading, (b) maximum fatigue loading and (c) minimum fatigue loading ( $R = 10$ ,  $P_N = 20 \text{ MPa}$ ,  $\sigma_{\text{fatigue}} = 300 \text{ MPa}$ ,  $\Delta l = 1.0 \text{ mm}$ ) 141
- 4.17 Predicted contact pressure distribution under different bone elastic modulus for (a) normal loading, (b) maximum fatigue loading and (c) minimum fatigue loading ( $R = -1$ ,  $P_N = 20 \text{ MPa}$ ,  $\sigma_{\text{fatigue}} = 300 \text{ MPa}$ ,  $\Delta l = 1.0 \text{ mm}$ ) 143
- 4.18 Predicted contact slip distribution under different bone elastic modulus for (a) normal loading, (b) maximum fatigue loading and (c) minimum fatigue loading ( $R = -1$ ,  $P_N = 20 \text{ MPa}$ ,  $\sigma_{\text{fatigue}} = 300 \text{ MPa}$ ,  $\Delta l = 1.0 \text{ mm}$ ) 144





- 4.19 Effect of delamination length on maximum contact pressure under different stress ratio for (a) normal loading, (b) maximum fatigue loading and (c) minimum fatigue loading ( $E_{\text{bone}} = 1 \text{ GPa}$ ,  $P_N = 20 \text{ MPa}$ ,  $\sigma_{\text{fatigue}} = 300 \text{ MPa}$ ) 146
- 4.20 Effect of delamination length on maximum contact slip under different stress ratio for (a) normal loading, (b) maximum fatigue loading and (c) minimum fatigue loading ( $E_{\text{bone}} = 1 \text{ GPa}$ ,  $P_N = 20 \text{ MPa}$ ,  $\sigma_{\text{fatigue}} = 300 \text{ MPa}$ ) 147
- 4.21 Effect of loading condition on maximum contact pressure under different stress ratio for (a) normal loading, (b) maximum fatigue loading and (c) minimum fatigue loading ( $E_{\text{bone}} = 1 \text{ GPa}$ ,  $\text{Del} = 1.0 \text{ mm}$ ) 149
- 4.22 Effect of loading condition on maximum contact slip under different stress ratio for (a) normal loading, (b) maximum fatigue loading and (c) minimum fatigue loading ( $E_{\text{bone}} = 1 \text{ GPa}$ ,  $\text{Del} = 1.0 \text{ mm}$ ) 150
- 4.23 Effect of bone elastic modulus on maximum contact pressure under different stress ratio for (a) normal loading, (b) maximum fatigue loading and (c) minimum fatigue loading ( $P_N = 20 \text{ MPa}$ ,  $\sigma_{\text{fatigue}} = 300 \text{ MPa}$ ,  $\text{Del} = 1.0 \text{ mm}$ ) 151
- 4.24 Effect of bone elastic modulus on maximum contact slip under different stress ratio for (a) normal loading, (b) maximum fatigue loading and (c) minimum fatigue loading ( $P_N = 20 \text{ MPa}$ ,  $\sigma_{\text{fatigue}} = 300 \text{ MPa}$ ,  $\text{Del} = 1.0 \text{ mm}$ ) 153
- 4.25 Schematic of delamination process at HAp-Ti-6Al-4V interface 154
- 4.26 Predicted interface damage under different loading condition for (a) normal loading, (b) maximum



	fatigue loading and (c) minimum fatigue loading ( $R = 0.1$ and $E_{bone} = 1$ GPa)	156
4.27	Predicted interface damage under different loading condition for (a) normal loading, (b) maximum fatigue loading and (c) minimum fatigue loading ( $R = 10$ and $E_{bone} = 1$ GPa)	158
4.28	Predicted interface damage under different loading condition for (a) normal loading, (b) maximum fatigue loading and (c) minimum fatigue loading ( $R = -1$ and $E_{bone} = 1$ GPa)	159
4.29	Predicted interface damage under different bone elastic modulus for (a) normal loading, (b) maximum fatigue loading and (c) minimum fatigue loading ( $R = 0.1$ , $P_N = 20$ MPa and $\sigma_{fatigue} = 500$ MPa)	162
4.30	Predicted interface damage under different bone elastic modulus for (a) normal loading, (b) maximum fatigue loading and (c) minimum fatigue loading ( $R = 10$ , $P_N = 20$ MPa and $\sigma_{fatigue} = 500$ MPa)	163
4.31	Predicted interface damage under different bone elastic modulus for (a) normal loading, (b) maximum fatigue loading and (c) minimum fatigue loading ( $R = -1$ , $P_N = 20$ MPa and $\sigma_{fatigue} = 500$ MPa)	165
4.32	Effect of loading condition on delamination length under different stress ratio for (a) normal loading, (b) maximum fatigue loading and (c) minimum fatigue loading ( $E_{bone} = 1$ GPa)	167
4.33	Effect of bone elastic modulus on delamination behaviour under different stress ratio for (a) normal loading, (b) maximum fatigue loading and (c) minimum fatigue loading ( $P_N = 20$ MPa and $\sigma_{fatigue} = 500$ MPa)	169
4.34	Predicted interface damage under different interface strength for stress ratio (a) $R = 0.1$ , (b) $R = 10$ and (c) $R = -1$	171



4.35	Predicted interface damage under different interface stiffness for stress ratio (a) $R = 0.1$ , (b) $R = 10$ and (c) $R = -1$	174
4.36	Predicted interface damage under different interface energy release rate for stress ratio (a) $R = 0.1$ , (b) $R = 10$ and (c) $R = -1$	176
4.37	Effect of interface strength on delamination initiation behaviour under different stress ratio ( $P_N = 20$ MPa, $\sigma_{\text{fatigue}} = 550$ MPa and $E_{\text{bone}} = 1$ GPa)	177
4.38	Effect of interface stiffness on delamination behaviour under different stress ratio $P_N = 20$ MPa, $\sigma_{\text{fatigue}} = 550$ MPa and $E_{\text{bone}} = 1$ GPa)	179
4.39	Effect of interface energy release rate on delamination behaviour under different stress ratio	180
4.40	Schematic of delamination-fretting wear process at HAp-Ti-6Al-4V interface	181
4.41	Predicted delamination-fretting wear under different delamination length for stress ratio (a) $R = 0.1$ , (b) $R = 10$ and (c) $R = -1$	183
4.42	Predicted delamination-fretting wear under different loading condition for stress ratio (a) $R = 0.1$ , (b) $R = 10$ and (c) $R = -1$	185
4.43	Predicted delamination-fretting wear under different bone elastic modulus for stress ratio (a) $R = 0.1$ , (b) $R = 10$ and (c) $R = -1$	187
4.44	Predicted delamination-fretting wear under different cycle number for stress ratio (a) $R = 0.1$ , (b) $R = 10$ and (c) $R = -1$	190
4.45	Predicted evolution of (a) contact pressure and (b) contact slip under different cycle number ( $R = 0.1$ , $\Delta \ell = 1.0$ mm, $P_N = 30$ MPa, $\sigma_{\text{fatigue}} = 250$ MPa and $E_{\text{bone}} = 1$ GPa)	192



4.46	Effect of delamination length on maximum wear depth under different stress ratio ( $P_N = 20$ MPa, $\sigma_{\text{fatigue}} = 300$ MPa, $E_{\text{bone}} = 1$ GPa and $N = 1,000,000$ )	193
4.47	Effect of loading condition on maximum wear depth under different stress ratio ( $\text{Del} = 1.0$ mm, $E_{\text{bone}} = 1$ GPa and $N = 1,000,000$ )	194
4.48	Effect of bone elastic modulus on maximum wear depth under different stress ratio ( $\text{Del} = 1.0$ mm, $P_N = 20$ MPa, $\sigma_{\text{fatigue}} = 300$ MPa and $N = 1,000,000$ )	195
4.49	Effect of cycle number on maximum wear depth under different stress ratio ( $\text{Del} = 1.0$ mm, $P_N = 20$ MPa, $\sigma_{\text{fatigue}} = 300$ MPa and $E_{\text{bone}} = 1$ GPa)	197
4.50	Multiple regression analysis output for stress ratio, $R = 0.1$	199
4.51	Multiple regression analysis output for stress ratio, $R = 10$	200
4.52	Multiple regression analysis output for stress ratio, $R = -1$	202
4.53	Multiple regression analysis output for combined stress ratio, $R = 0.1, 10$ and $-1$	204
4.54	Actual versus predicted max wear depth scattered plot	205



## LIST OF SYMBOLS AND ABBREVIATIONS

$E_d$	-	Accumulated dissipated energy
$\Delta$	-	Opening displacement
$\Delta h$	-	Wear depth
$\mu$	-	Friction coefficient
$\mu m$	-	Micrometre
$a$	-	Half-width length
$b$	-	Coefficient
$E$	-	Elastic modulus
$E^*$	-	Combined elastic modulus
$E_{bone}$	-	Bone elastic modulus
$F$	-	Normal load
$G_N^c$	-	Normal energy release rate
$G_T^c$	-	Shear energy release rate
$H$	-	Hardness
$k$	-	Coefficient of wear
$K$	-	Dimensionless wear coefficient
$K_c$	-	Stress intensity factor
$K_N$	-	Normal interfacial stiffness
$K_T$	-	Shear interfacial stiffness
$N$	-	Newton
$N$	-	Number of cycles
$p(x)$	-	Contact pressure distribution
$P_0$	-	Maximum contact pressure
$P_m$	-	Flow pressure
$P_N$	-	Normal load
$R$	-	Curvature radius
$R^*$	-	Combined radius



PTT AUTHM  
 PERPUSTAKAAN TUNKU TUN AMINAH

$rpm$	-	Rotation per minute
$S$	-	Sliding distance
$t$	-	Specific time
$t_N^0$	-	Normal interfacial strength
$t_t^0$	-	Shear interfacial strength
$U2$	-	Spatial displacement of nodes in vertical direction
$\nu$	-	Poisson's ratio
$V$	-	Wear volume
$W$	-	Total work done
$x$	-	Horizontal length
$x$	-	Independent variable
$y$	-	Dependent variable
$\alpha$	-	Dundur's first parameter
$\delta$	-	Amplitude of displacement
$\Delta K$	-	Kinetic energy
$\Delta N$	-	Cycle jump
$\Delta U$	-	Potential energy
$\pi$	-	Phi
$\sigma$	-	Interface traction
$\sigma_{fatigue}$	-	Fatigue load
$R$	-	Stress ratio
$2D$	-	Two-dimensional
$3D$	-	Three-dimensional
$ALE$	-	Arbitrary Lagrangian-Eulerian
$CNC$	-	Computer numerical control
$CoC$	-	Ceramic-on-ceramic
$COF$	-	Coefficient of friction
$CoP$	-	Ceramic-on-plastic
$CPRESS$	-	Contact pressure
$CSLIP$	-	Contact slip
$CZM$	-	Cohesive zone modelling
$Del$	-	Delamination
$ETP$	-	Economic Transformation Programme
$FE$	-	Finite element



PTTA UTHM  
PERPUSTAKAAN TUNKU TUN AMINAH

<i>FEM</i>	-	Finite element method
<i>GPa</i>	-	Gigapascal
<i>GTP</i>	-	Government Transformation Programme
<i>HAp</i>	-	Hydroxyapatite
<i>HXLPE</i>	-	Highly cross-linked polyethylene
<i>LEFM</i>	-	Linear elastic fracture mechanics
<i>mm</i>	-	Millimetre
<i>MoM</i>	-	Metal-on-metal
<i>MoP</i>	-	Metal-on-plastic
<i>MPa</i>	-	Megapascal
<i>NEM</i>	-	National New Economic Model
<i>NKEA</i>	-	National Key Economic Area
<i>NUT</i>	-	Nagaoka University of Technology
<i>ODB</i>	-	Output database
<i>PP</i>	-	Polypropylene
<i>PU</i>	-	Polyurethane
<i>SBF</i>	-	Simulated body fluid
<i>SDEG</i>	-	Stiffness degradation
<i>SEM</i>	-	Scanning electron microscope
<i>SRI</i>	-	Strategic Reform Initiatives
<i>THR</i>	-	Total hip replacement
<i>Ti</i>	-	Titanium
<i>Ti-6Al-4V</i>	-	Titanium alloy
<i>TSL</i>	-	Traction-separation law
<i>TTS</i>	-	Tribologically transformed structure
<i>UHMWPE</i>	-	Ultra-high-molecular-weight polyethylene
<i>UTHM</i>	-	Universiti Tun Hussein Onn Malaysia
<i>VCCT</i>	-	Virtual crack closure technique
<i>XFEM</i>	-	Extended finite element method



PERPUSTAKAAN TUN AMINAH  
 PTTA UTHM

**LIST OF APPENDICES**

<b>APPENDIX</b>	<b>TITLE</b>	<b>PAGE</b>
A	ABAQUS UMESHMOTION Subroutine	228
B	Stress Ratio, $R = 0.1$ data set	234
C	Stress Ratio, $R = 10$ data set	238
D	Stress Ratio, $R = -1$ data set	242
E	Stress Ratio, $R = 0.1, 10$ and $-1$ (combined) data set	246



PT TA UTHIM  
PERPUSTAKAAN TUNKU TUN AMINAH



## CHAPTER 1

### INTRODUCTION

#### 1.1 Background of study

Hip joint is one of the important synovial ball and socket joints which connecting femur with pelvis in human body (Abd-elsayed, 2019). Basically, hip joint is made up of femoral head (ball) and acetabulum (socket) as shown in Figure 1.1. The hip joint transmits load from lower limb through the pelvis to the axial skeleton. However, hip diseases are prone to occur due to injuries, infections, chronic conditions and developmental conditions. Osteoarthritis, inflammatory arthritis, bone fracture, slipped capital femoral epiphysis, abnormal developmental conditions, soft tissue pain and perthes disease are among the common hip disorders (Fallahnezhad, 2018).

Osteoarthritis is the most common form of hip disorders that affecting millions of people around the globe. Osteoarthritis is a condition where the protective cartilage that cushions at hip ball and socket joint is worn out over time as illustrated in Figure 1.2. The deterioration of protective cartilage will cause bone rubbing on bone and worsening of connective tissues/muscles at hip joint. Osteoarthritis is one of the critical hip disorders, especially in developed countries due to rapid aging population (Otsuka *et al.*, 2016). In fact, osteoarthritis is a degenerative disorder that worsens over time and can lead to several complications such as chronic joint pain, immobility and disability. Thus, total hip replacement (THR) surgery is required to replace damaged or worn out hip joints. Damaged protective cartilage and femoral head of hip joint are removed and replaced with hip prosthetic components (artificial hip implants) which made up of acetabular cup, plastic inner, femoral head and stem which connecting pelvis with femur as shown in Figure 1.2.

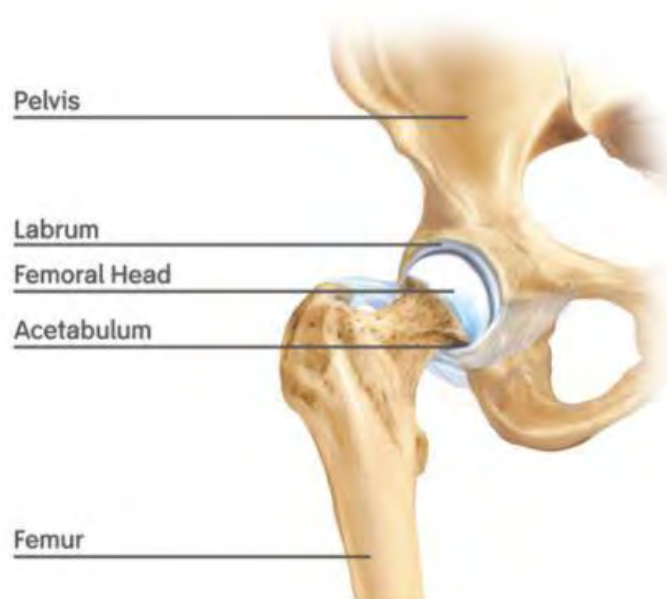


Figure 1.1: Hip joint anatomy (Fallahnezhad, 2018)

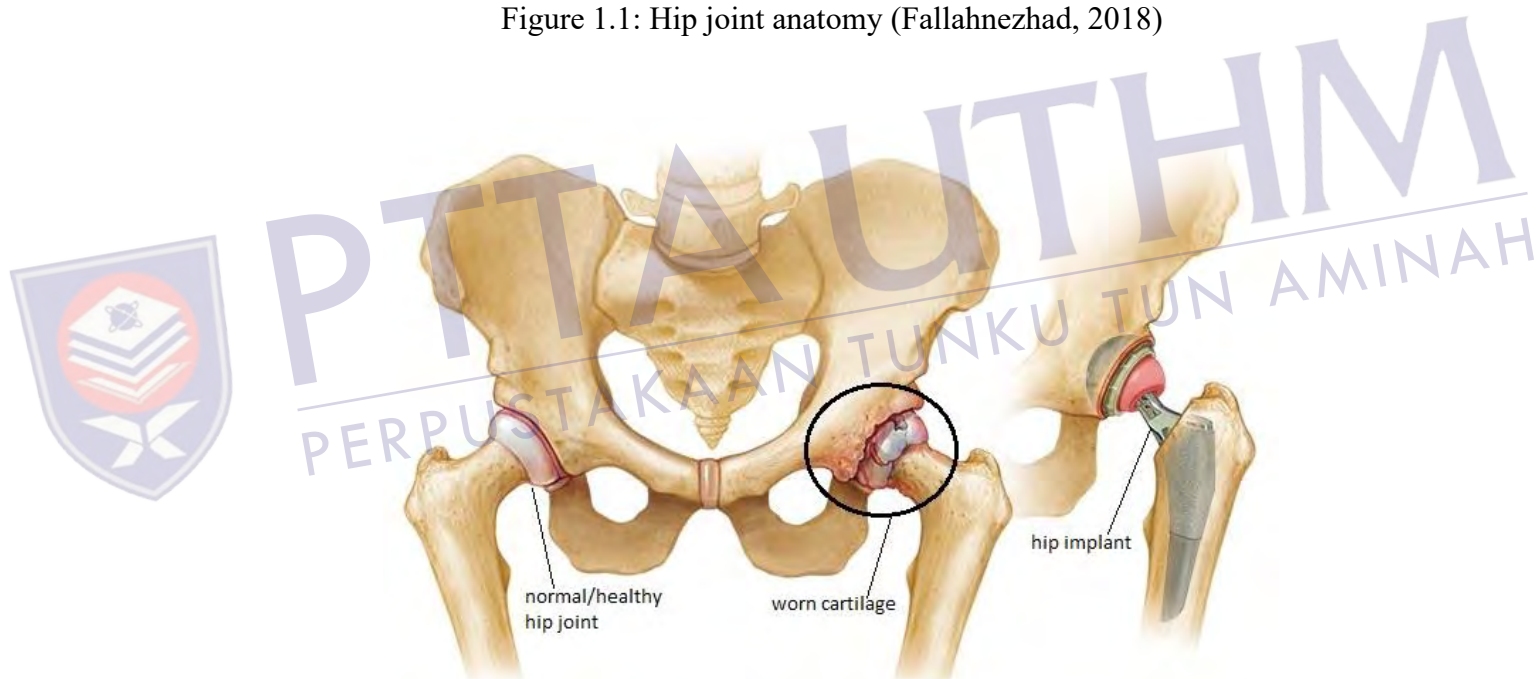


Figure 1.2: Osteoarthritis and total hip replacement (THR) surgery (Fallahnezhad, 2018)

The Australian Orthopaedic Association National Joint Replacement Registry (Graves *et al.*, 2004; System, 2019) has reported that 88.8 % of total hip replacement (THR) surgery is attributable to osteoarthritis condition.

Artificial hip implants utilised in total hip replacement (THR) surgery is normally made of titanium alloys (Ti-6Al-4V). The extensive application of titanium

alloys (Ti-6Al-4V) in biomechanics field mainly as artificial hip implant is predominant due to its low weight, high strength and corrosion resistance characteristics (Nagentrau *et al.*, 2019). However, titanium alloys (Ti-6Al-4V) cannot directly adhere to human bone due to biocompatibility issue (Nagentrau *et al.*, 2020). Thus, bonds/coating that having similar properties of bone minerals is necessary to increase bone bonding ability with titanium (Ti-6Al-4V) artificial hip implants. Hydroxyapatite (HAp:Ca<sub>10</sub>(PO<sub>4</sub>)(OH)<sub>2</sub>), a bio-ceramics material which contains main composition of human bone is broadly used to promote bonds between bone and titanium (Ti-6Al-4V) artificial hip implants (Otsuka *et al.*, 2016).

Hydroxyapatite (HAp) coating is deposited on Ti-6Al-4V artificial hip implant femoral stem by plasma spraying technique. Practically, Hydroxyapatite (HAp) coated Ti-6Al-4V artificial hip implant femoral stem can achieve good fixation with human bone upon completion of subsequent adhesion due to bone ingrowth process. On the other hand, Hydroxyapatite (HAp) coating is susceptible to fail due to fatigue cracks, brittle fracture, delamination and fretting wear (Otsuka *et al.*, 2016). Consequently, the effectiveness of Hydroxyapatite (HAp) coating is greatly challenged in long term usage more than 10 years. Hydroxyapatite (HAp) coating can experience coating through thickness crack (vertical crack) due to fretting fatigue as results of gait cycle.

Hydroxyapatite (HAp) coating interfacial delamination is initiated as coating through thickness crack (vertical crack) reached until the interfaces of HAp-Ti-6Al-4V and HAp-human bone respectively. The coating delamination condition can lead to relative contact slip which accelerating fretting wear behaviour at interfaces. Figure 1.3 presents the delamination-fretting wear mechanism at hip implants. Wear particles are formed from delamination-fretting wear mechanism able to activate inflammations at surrounding organs, which causes implant loosening and subsequent failures (Nagentrau *et al.*, 2019). Thus, such a condition can increase the risk of artificial hip implant revision surgery.

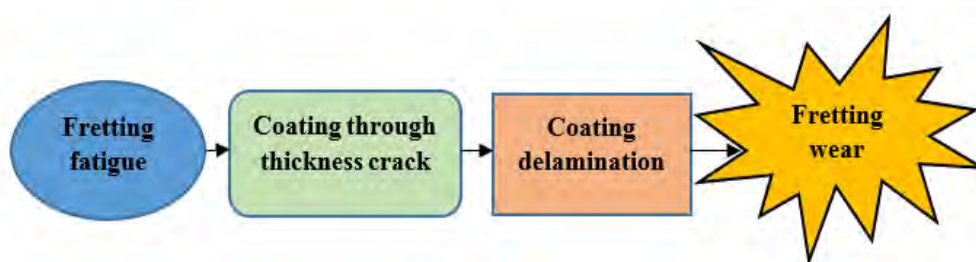


Figure 1.3: Delamination-fretting wear failure mechanism (Nagentrau *et al.*, 2019)

However, to the best of authors knowledge, far too little attention has been paid to combined delamination and fretting wear behaviours at artificial hip implant femoral stem part that can suitably mimic actual loading conditions. In fact, most of the open literatures are focussing on failure behaviour at acetabular cup (ball-socket interface) and very limited studies are considering artificial hip implant femoral stem part (English *et al.*, 2015; Fallahnezhad *et al.*, 2017; Otsuka *et al.*, 2016). Therefore, this research aims to develop a delamination-fretting wear finite element model to formulate maximum wear depth predictive equation as a novel and fast failure prediction tool. In addition, present research addresses contact pressure, contact slip, interface damage, delamination initiation and delamination-fretting wear behaviours at HAp-Ti-6Al-4V interface of artificial hip implant femoral stem component by adopting finite element approach using contact modelling, cohesive zone modelling (CZM) and adaptive wear modelling (UMESHMOTION subroutine) respectively. The influence of delamination length, loading condition, bone elastic modulus, stress ratio, number of cycles along with interfacial properties are among the focus of present study.

## 1.2 Problem statement

Artificial hip implant failure is commonly occurring at acetabular cup (ball-socket interface) and femoral stem region. Research on delamination and fretting wear in artificial hip implant has been carried out for many years. However, far too little attention has been paid to femoral stem region and in-depth research are required to investigate delamination and fretting wear failure behaviour at that region. Previous researchers have explored cyclic delamination of plasma sprayed Hydroxyapatite

(HAp) coating and its effect on fretting wear behaviour. However, no study has been examined combined delamination-fretting wear behaviour at artificial hip implant femoral stem component. Delamination of Hydroxyapatite (HAp) coating due to coating through thickness crack (vertical crack) initiated by fretting fatigue can promote fretting wear behaviour in femoral stem region of artificial hip implant (Nagentrau *et al.*, 2019; Otsuka *et al.*, 2016). In fact, there is absence of combined delamination-fretting failure prediction model that could suitably mimic actual loading conditions at HAp-Ti-6Al-4V interface accurately. This clearly shows that limited attempt has been done to explore the potential of developing a reliable combined delamination-fretting wear failure prediction model. It appears from the reported literatures that most attention has been paid to experimental work and it is essential to develop a finite element model to perform detailed parametric studies at HAp-Ti-6Al-4V interface. Combined delamination-fretting wear failure prediction model is very crucial for better design process of Hydroxyapatite (HAp) coated Ti-6Al-4V implants to minimize artificial hip implant in service failure. Besides that, research studies focussing the effect of mechanical and tribological properties of HAp-Ti-6Al-4V interface on delamination-fretting wear are still lacking in biomechanics field.

In fact, delamination-fretting wear possibly can occur at two artificial hip stem interfaces such as HAp-Ti-6Al-4V and HAp-human bone respectively (Otsuka *et al.*, 2016). HAp-Ti-6Al-4V interface solely focussed in present study rather than in HAp-human bone interface as Hydroxyapatite (HAp) coating able to achieve good fixation and subsequent adhesion with human bone once bone ingrowth. Thus, fretting wear particles generated in HAp-human bone interface will be suppressed. However, HAp-Ti-6Al-4V is considered as critical interface as fretting wear particles will be ejected and transported along the surrounding region as shown in Figure 1.4. Present study is designed to shed a light to explore the combined delamination-fretting wear behaviour at HAp-Ti-6Al-4V interface since no attempt has been done previously by other researchers.

In addition, the lack of new findings and advancement in fundamental knowledge about delamination-fretting wear failure behaviour using finite element methodology requires in-depth exploration. It should be noted that no attempt is done previously to develop a delamination-fretting wear model using finite element methodology to formulate maximum wear depth predictive equation as a novel and fast failure prediction tool which able to assist in reducing the amount of testing



required and better design process of Hydroxyapatite (HAp) coated artificial hip implant femoral stem component. Besides that, there have been no controlled studies which compare the influence delamination length, loading condition, bone elastic modulus, stress ratio, number of cycles along with interfacial properties on delamination-fretting wear behaviour to minimise associated failure because such a flaw is life threatening and also costly.

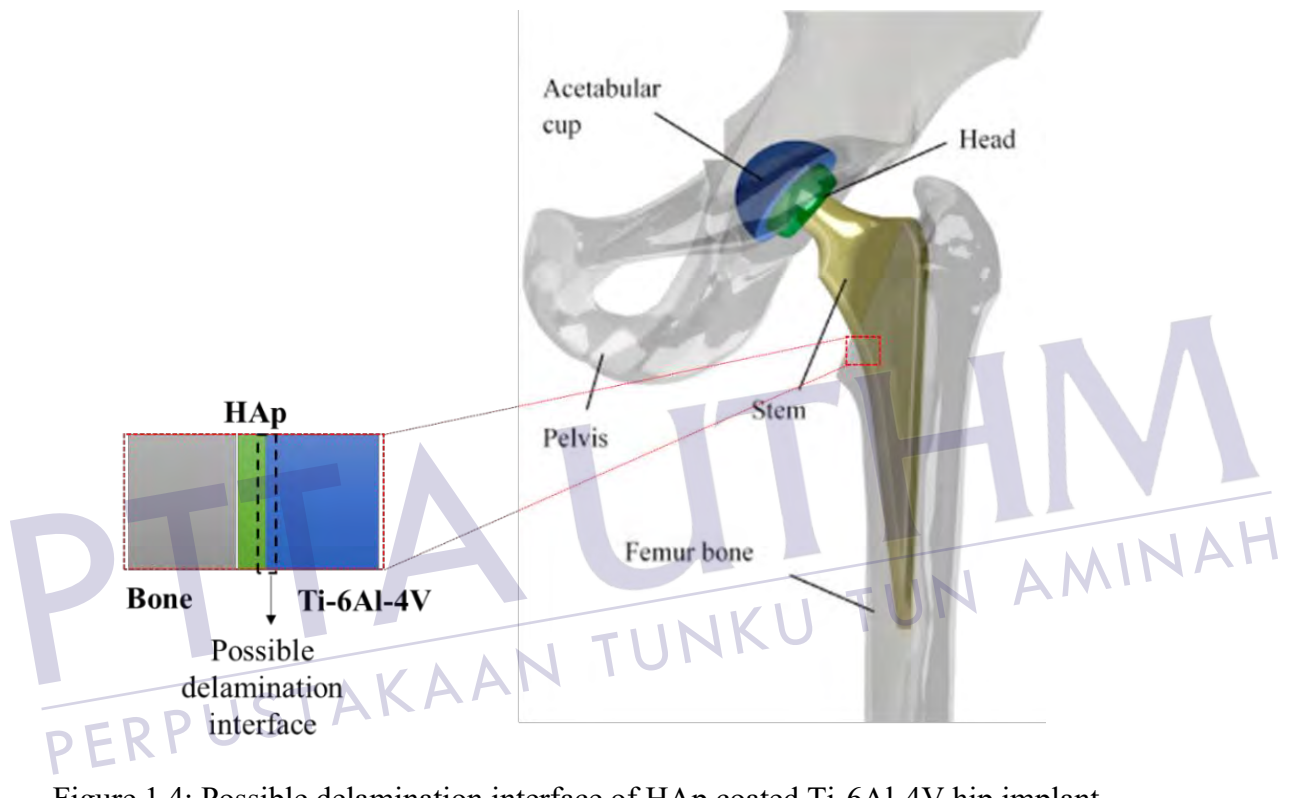


Figure 1.4: Possible delamination interface of HAp coated Ti-6Al-4V hip implant  
(English *et al.*, 2015)

### 1.3 Research questions

This research will contribute in enhancing knowledge about delamination-fretting wear behaviour at HAp-Ti-6Al-4V interface of hip implant femoral stem by imposing following research question:

- i. How does the different mechanical and tribological properties affect contact pressure and contact slip distribution at HAp-Ti-6Al-4V interface of artificial femoral stem component?
- ii. How does the different mechanical, tribological and interfacial properties such as interfacial stiffness, strength and energy release rate affect interface damage along with coating delamination at HAp-Ti-6Al-4V interface of artificial femoral stem component?
- iii. How does the finite element methodology can be implemented to perform detailed parametric studies and develop delamination-fretting wear model subjected to different mechanical and tribological properties to formulate maximum wear depth predictive equation using multiple linear regression as a novel and fast failure prediction tool at HAp-Ti-6Al-4V interface?

#### 1.4 Research objectives

The objectives of present research work are presented as follows:

- i. To develop finite element contact model of HAp-Ti-6Al-4V interface subjected to different mechanical and tribological properties to predict contact pressure and contact slip distribution.
- ii. To analyse HAp-Ti-6Al-4V interface damage and coating delamination initiation behaviour under different mechanical, tribological and interfacial properties using cohesive zone modelling (CZM).
- iii. To evaluate proposed delamination-fretting wear finite element model subjected to different mechanical and tribological properties to formulate maximum wear depth predictive equation as a novel and fast failure prediction tool.



PTTA UTHM  
PERPUSTAKAAN TUNJUKU TUN AMINAH

## 1.5 Research scopes and limitations

The scopes and limitations of the present research are established in order to achieve focused goals in line with research questions and aims. Hence, the scopes and limitations of this research are drawn as following:

- i. Modelling  $\frac{1}{4}$  symmetric two-dimensional (2D) plane strain case HAp coated Ti-6Al-4V based on fretting fatigue specimen to represent artificial hip implant femoral stem using ABAQUS commercial finite element software (version 6.13).
- ii. Modelling HAp coated Ti-6Al-4V substrate contact configuration subjected to normal and fatigue loading condition.
- iii. Ti-6Al-4V substrate and HAp coating are modelled as fully elastic bodies with elastic modulus of 110 GPa and 70 GPa respectively.
- iv. HAp coating thickness is modelled as 150  $\mu\text{m}$  representing plasma sprayed coating deposition.
- v. PU foam contact pad with elastic modulus of 0.1 - 1.0 GPa and 2.0 - 20.0 GPa are modelled to represent porous (cancellous) and cortical bones respectively.
- vi. Friction and wear coefficients at HAp-Ti-6Al-4V interface are modelled as 0.7 and  $2.0 \times 10^{-8}$  ( $\text{mm}^3/\text{N}\cdot\text{mm}$ ) respectively.
- vii. HAp coating vertical crack is applied by  $\frac{1}{4}$  symmetric modelling approach to represent coating through thickness crack until the interface to initiate delamination.
- viii. Evaluating concerned variables of fatigue loading (250 - 350 MPa), normal loading (20 - 30 MPa), delamination length (0.25 - 1.0 mm), stress ratio (0.1, 10, -1) and bone elastic modulus (0.1 - 20 GPa) at HAp-Ti-6Al-4V interface.
- ix. Only HAp-Ti-6Al-4V interface of artificial hip implant femoral stem component is focussed.
- x. Delamination length is controlled by implementing tie constraint technique during finite element contact and wear modelling.
- xi. Cycle jump technique with  $\Delta N = 1 \times 10^4$  is implemented during finite element wear modelling.
- xii. The developed delamination-fretting wear model can be utilised for delamination length ranging from 0.25 mm - 1.0 mm, normal loading of



20 MPa - 30 MPa with fatigue loading of 250 MPa - 350 MPa subjected to stress ratio,  $R = 0.1$ ,  $R = 10$  and  $R = -1$  and number of cycle up to 1,000,000.

### **1.6 Research novelty**

It appears from the aforementioned investigations that most attention has been paid to artificial acetabular cup (ball-socket interface) and very few studies examined artificial hip implant femoral stem component. Thus, present research is mainly focussing on the combined delamination-fretting wear behaviour at artificial hip implant femoral stem. Besides that, delamination-fretting wear behaviour at HAp-Ti-6Al-4V interface has not been considered before. Nevertheless, limited attempt has been done to explore the potential of developing a delamination-fretting wear behaviour model using finite element methodology to formulate maximum wear depth predictive equation as a novel and fast failure prediction tool. In addition, present research is hoped to shed some light in evaluating different mechanical and tribological properties such as delamination length, loading condition, bone elastic modulus, cycle number and stress ratio at HAp-Ti-6Al-4V interface and its response on contact pressure, contact slip, interface damage, delamination initiation and delamination-fretting wear behaviour.

### **1.7 Research significance**

The contribution of present research is obvious as resulting outcomes can be capitalised as guideline to evaluate artificial hip implant femoral stem failure associated with delamination and fretting wear through implementation of finite element methodology. In addition, the proposed finite element model can be easily accommodating different mechanical, tribological and interfacial properties of artificial femoral stem component HAp-Ti-6Al-4V interface to perform detailed parametric studies with minimal costly experimental works. The uniqueness of this research will be an advancement in fundamental understanding of delamination-fretting wear behaviour at HAp- Ti-6Al-4V interface.

The outcome of this research is a novel and fast failure prediction tool which can be used to better assist in maximum delamination-fretting wear depth prediction at artificial hip implant femoral stem component. The maximum delamination-fretting wear depth prediction tool will assist in reducing the amount of testing required and better design process of HAp coated hip implants. Besides that, accurate prediction and speedy assessment of delamination-fretting wear could contribute in improving service life of implants. Present research also relevant and inline to with Malaysian Sustainable Development Goals (SDG) focussing on Goal No. 3 and Goal No.4 which are Good Health and Well-being and Quality Education respectively. Besides that, present research also can be related to Science, Technology, Innovation & Commercialisation from Economic Empowerment pillar and Health & Education from Social Re-engineering pillar under Twelfth Malaysian Plan (RMK-12).

## 1.8 Thesis organisation

The outline of the thesis is presented as below:

**Chapter 1:** Presents research background, problem statement, research questions, objectives, scopes and limitation. In addition, novelty and significance of research also highlighted.

**Chapter 2:** Presents extensive literature review on anatomy of hip, artificial hip implant, contact mechanics of HAp coated Ti-6Al-4V addressing delamination and fretting wear failure, finite element contact modelling, cohesive zone modelling and wear modelling. The research gap is identified towards the end of literature review.

**Chapter 3:** Outlines whole methodology including contact modelling, cohesive zone modelling (CZM) and wear modelling using finite element methodology to develop novel and fast failure prediction tool.

**Chapter 4:** Evaluates influence of different mechanical and tribological properties such as delamination length, loading condition, bone elastic modulus, cycle number



and stress ratio on contact pressure, contact slip, interface damage, delamination initiation and delamination-fretting wear behaviour at HAp-Ti-6Al-4V interface of artificial hip implant femoral stem.

**Chapter 5:** Draws conclusion and knowledge contribution of present work with .  
recommendation for future works.



PTTA UTHM  
PERPUSTAKAAN TUNKU TUN AMINAH

## CHAPTER 2

### LITERATURE REVIEW

#### 2.1 Introduction

In this chapter, the overview of total hip replacement (THR) using artificial hip implant is highlighted to firmly understand contact mechanics associated failures. In addition, HAp coated artificial femoral stem failure due to fretting condition is discussed in detail. HAp-Ti-6Al-4V interface delamination and fretting wear experimental studies are focussed. Apart from that, cohesive zone modelling and fretting wear modelling approaches to predict delamination and fretting wear behaviour are reviewed comprehensively. Based on the literature review, several research gaps are identified to be addressed in present study.

#### 2.2 Anatomy of hip joint

Hip joint is basically ball and socket connection which made up of femoral head (ball) and acetabulum (socket) (Hongyu & Blunt, 2009). Although, hip joint is stable to bear more weight but only can carry less range of motion compared to other ball-socket joints in human body such as shoulder joint (English *et al.*, 2015). Human hip joint comprises several parts i.e. femur bone head, acetabulum, joint capsule/ligaments, cartilage and tendons as illustrated in Figure 2.1. In fact, the human hip joint is supported with tendons, ligaments and muscles.

The human hip joint is enclosed by ligaments (joint capsule) which assists in stabilising hip motion during human activities. This thick ligament (joint capsule) contains pubofemoral, ischiofemoral and ilofemoral ligaments which located near ligamentum teres and labrum as shown in Figure 2.1. In addition, these ligaments cover femur head cartilages along with acetabulum. The thigh bone or femur is the heaviest, longest and strongest bone in human body (English *et al.*, 2015). The main function of femur is to transmit and support body weight during various human activities. It is noteworthy to mention that femur is always exposed to extreme force and can be stabilised with attached muscles strength. Meanwhile, acetabulum is a cup dented in the pelvis (concave surface). The hip joint is formed when pelvis and femur head is connected at this concave surface.

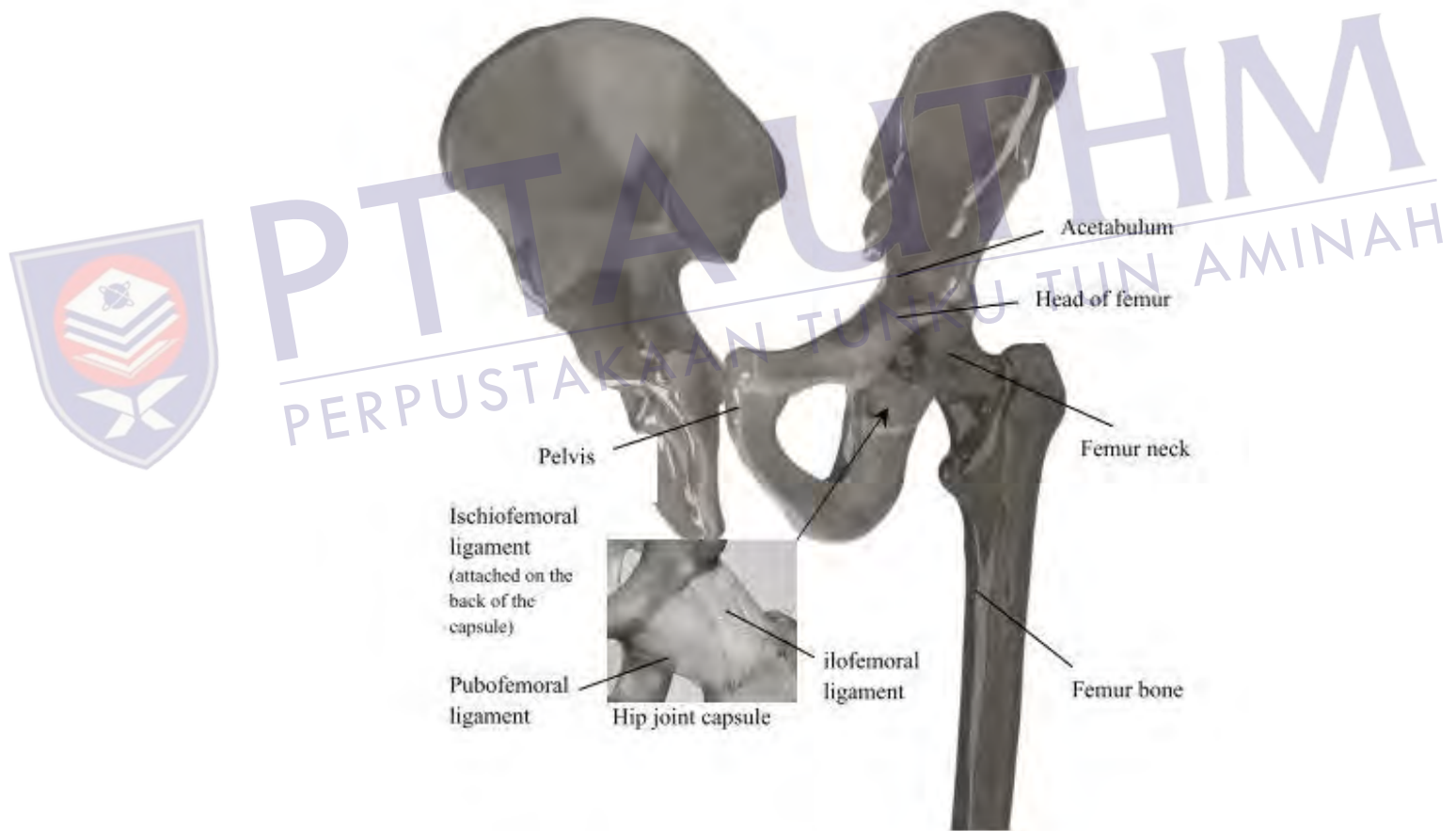


Figure 2.1: Human hip joint anatomy (English *et al.*, 2015)

Cartilage on femur head and acetabulum is responsible to lubricate the joint by providing smooth surface with the purpose of facilitate smooth or nearly frictionless motion. From a mechanical perspective it acts in similar manner as lubricant in

machineries. The human hip joint performance can be affected if damaged due to bone disease, overweight, overuse and others. Furthermore, the damaged or worn out cartilage can lead to articulation of high friction as hard bone surfaces such as femur head and acetabulum contact upon each other (English *et al.*, 2016). This condition will be causing high stresses and results in making the hip joint stiffer and painful.

### 2.3 Hip joint disorders

Human hip joint can transmit significant dynamic loads and extensive range of movement during human activities. The ability of hip joint in carrying and transmitting loads to provide mobility is remarkable. However, it is susceptible to deterioration and functional loss due to certain types of hip joint disorders. Hip joint can experience osteoarthritis, rheumatoid arthritis, avascular necrosis, trauma and bone fracture (English *et al.*, 2016). Osteoarthritis is a common and high-risk hip disorder due to worn cartilages which causing femur head and acetabulum bone contact each other and results in stiffness, immobility and chronic pain (Loeser, 2006).

Rheumatoid arthritis is a disorder where human suffer because of hip joint ligaments damage and bone erosion. Meanwhile, a condition of limited blood supply at joint tissue which leads to organ cells death in femur bone top region is known as avascular necrosis. This hip disorder can change bone shape, joint stiffness, loss of movement range and pain (English *et al.*, 2015). Besides that, trauma and bone fracture can be arisen due to sudden impact or fall and medical complication such as stress injuries, cancer and osteoporosis which weaken the bone and susceptible to fracture.

Physiotherapy and drugs can aid in reducing pain for patients experiencing hip joint disorders. However, effective treatment such as affected hip joint replacement is required to eliminate chronic pain in severe hip joint disorder cases. Total hip replacement (THR) is key solution to restore mobility and normal lifestyle of hip disorder patients as shown in Figure 2.2. Among all the hip disorders, Osteoarthritis is the principal cause for total hip replacement surgery as reported in The Australian Orthopaedic Association National Joint Replacement Registry (Graves *et al.*, 2004).



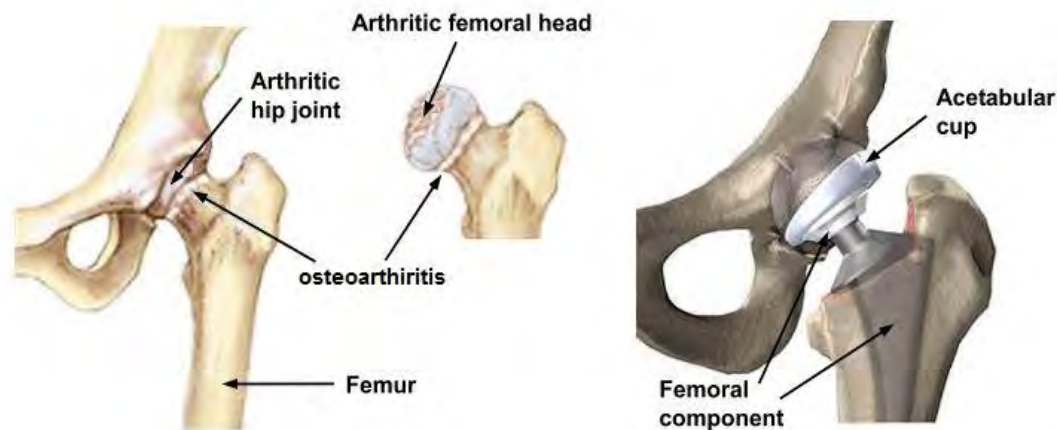


Figure 2.2: Osteoarthritis and total hip replacement (THR) surgery (Hongyu & Blunt, 2009)

#### 2.4 Total hip replacement (THR) using artificial hip implant

Total hip replacement surgery is most effective orthopaedic surgery performed worldwide with the aim of dramatically enhance mobility and life of patients suffering from hip related disorders such as osteoarthritis (Hongyu & Blunt, 2009). Total hip replacement (THR) surgery is commonly carried out using metallic artificial implant. Such a metallic artificial implants normally made up of Titanium alloys (Ti-6Al-4V) due to its interesting properties (Nagentrau *et al.*, 2019; Otsuka *et al.*, 2016). Titanium alloys (Ti-6Al-4V) is a high interest material in engineering application due to their low weight, excellent corrosion resistance, high ductility and fatigue resistance characteristics (Nagentrau *et al.*, 2016; Nagentrau *et al.*, 2015; Siswanto *et al.*, 2016; Siswanto *et al.*, 2015).

Total hip replacement surgery can bring immediate relief to patients who experiencing unremitting pain. In fact, this surgical procedure performed as a last attempt to relief pain and improve mobility of hip disorder patients. The very first total hip replacement is performed by Sir John Charnley (1911-1982) in November 1962 by replacing entire hip joint with metallic artificial implant and established surgical approach of implantation. The implantation foundation proposed by Charnley leads to advancement in surgical technique to facilitate active lifestyle of patients in present day. Artificial hip implant is a ball and socket joint which comprising femoral head, acetabular cup and femoral stem as shown in Figure 2.3.

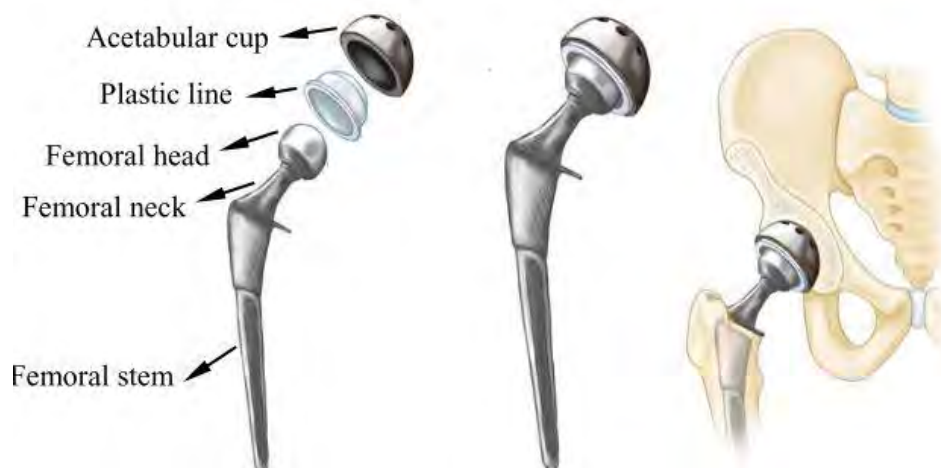


Figure 2.3: Artificial hip implant parts (English *et al.*, 2015)

There are two types of hip implant fixation approach as illustrated in Figure 2.4 to secure metallic femoral stem into femur such as cemented and uncemented total hip replacement respectively. Acrylic bone cement is utilised during metallic implant fixation to act as an intermediary agent stabilising femoral stem and transferring loading in cemented total hip replacement. Meanwhile a porous bio ceramic coating is applied on artificial femoral stem surface to enhance bone ingrowth in uncemented total hip replacement. Generally, bonds between metallic titanium alloy and bone are required as both cannot adhere directly (Laonapakul *et al.*, 2012).

Acetabular cup is fixed into artificial femoral stem in similar way under both uncemented and cemented total hip replacement (THR) techniques. The acetabular cup is held by fit tightness or with screws in uncemented THR, whereas bone cement is utilised to stabilise acetabular cup in cemented THR. The fixation method of THR using cemented or uncemented is highly personal and different according to counties and surgeons. For instance, national variations across the Europe ranges from 91% cemented THR in United Kingdom to 10% in Austria (Graves *et al.*, 2004). The combination of uncemented acetabular cup and cemented femoral stem is known as Hybrid THR which becoming popular in treating elderly patients (50 - 60 years old) in present day. However, the present research is focuses on uncemented THR where Hydroxyapatite (HAp) coating is plasma sprayed on metallic femoral stem.



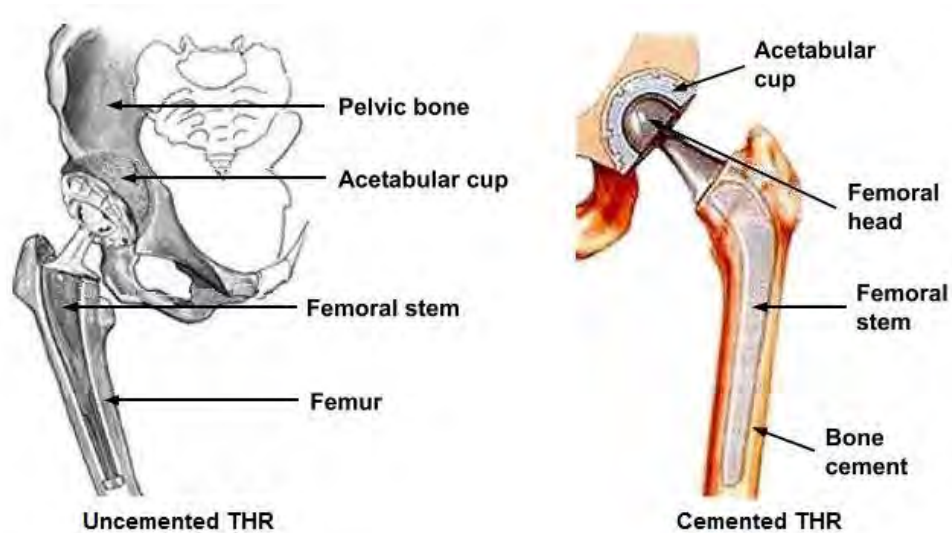


Figure 2.4: Uncemented and cemented total hip replacement (THR) (Hongyu & Blunt, 2009)

## 2.5 Hydroxyapatite (HAp) coated uncemented THR

Despite prior evidence, debates still ongoing concerning the ideal choice of total hip replacement (THR) fixation methods i.e. cemented THR and uncemented THR. The primary goal of uncemented THR is to enhance long term success in younger patients (Hongyu & Blunt, 2009). Ideally, Hydroxyapatite (HAp) coating is applied on Ti-6Al-4V metallic femoral stem in order to achieve osseointegration by promoting bone ingrowth. Potential benefits of HAp coated femoral stem fixation are capability of remodel activity and self-restoration over time.

Hydroxyapatite (HAp) ( $\text{Ca}_5(\text{PO}_4)_3(\text{OH})$ ) is broadly used as bio ceramic material because of its exceptional compatibility with bone (Lindahl, 2012). HAp coating is having similar properties with bone minerals. Several researchers have revealed that HAp coating is utilised as autogenous free bone grafting substance for past 30 years. In fact, it is most promising bioactive ceramics that widely used in orthopaedic, alveolar ridge, dental implants and scaffolds for bone growth during surgery (Haibo Wang, 2004). Plasma sprayed HAp coating on femoral stem surface forming textured or irregular surface for better mechanical interlock is fixed as shown in Figure 2.5.

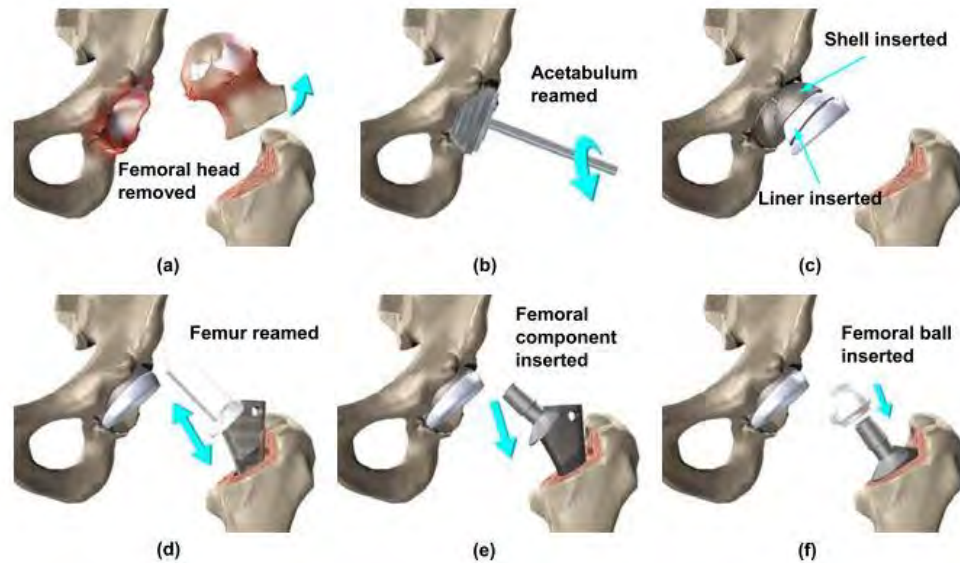


Figure 2.5: Typical procedures of HAp coated uncemented THR (Hongyu & Blunt, 2009)

## 2.6 Material of artificial hip implant

The material utilised to manufacture artificial hip implants should be biocompatible to reduce rejection risk and minimise toxicity. The increase in number of young patients using artificial hip implant has maximise application of bearing materials. The material characteristics of artificial hip implant components play a vital role in improving durability as human body environment is highly corrosive (English *et al.*, 2015). The components material of artificial hip implant in total hip replacement (THR) surgery is as below:

**Acetabular cup:** The acetabular cup which held into pelvis or bearing surface is typically fabricated from Ultra-High-Molecular-Weight Polyethylene (UHMWPE). UHMWPE is an appealing material due to its low wear rate, low friction, good impact resistance, high toughness and good biocompatibility characteristics. Besides that, Highly Cross-linked Polyethylene (HXLPE), alumina ceramics, zirconia ceramics and cobalt-chrome alloy are also common materials to manufacture acetabular cup (English *et al.*, 2016).

**Femoral head:** Artificial hip implant femoral head are commonly manufactured using cobalt-chrome alloys, stainless steel (high grade) and ceramic. Cobalt-chrome alloys usually compatible with UHMWPE acetabular cup besides displaying superior corrosion resistance, reduced inflammation, high wear resistance, high hardness and excellent biocompatibility characteristics. Thus, it enables comparatively successful performance to be utilised in orthopaedic application (Brown & Lemons, 1996; Kohn, 1998). In addition, ceramic material also suitable for femoral head due to its low friction which can reduce wear rate and wear debris.

**Modular stem:** Artificial hip modular stem which fixed into femur bone medullary cavity is made up of titanium alloys (Ti-6Al-4V). Ti-6Al-4V is low weight high strength material compared to other orthopaedic alloys (Apostu *et al.*, 2018; Fokter *et al.*, 2017). In addition, Ti-6Al-4V alloy exhibiting good tissue tolerance, high wear and corrosion resistance. Cobalt-chrome alloy or stainless steel also used to fabricate modular stem but very seldom (Malahias *et al.*, 2020).

Different materials are combined to manufacture artificial hip implant components to achieve different interfacial properties. Material combination term is basically referring to bearing material combination in acetabular cup and femoral head. There are numerous material combinations for surface articulation in manufacturing artificial hip implants i.e. Ceramic-on-plastic (CoP), Metal-on-Plastic (MoP), Metal-on-Metal (MoM) and Ceramic-on-Ceramic (CoC).

**CoP and MoP:** High cross-linked Polyethylene and UHMWPE are common plastics employed in CoP and MoP application due to high wear resistance compared to other types of plastics. However, it exhibits high wear rate if compared with ceramic and metal materials (English *et al.*, 2015). UHMWPE plastic permits the usage of larger femoral head and perform well as good shock absorber to allow greater mobility during human activities.

**CoC:** This category of artificial hip implant protects the surface by minimising scratch possibilities and ensure couples experience limited deterioration due to wear. In fact, CoC displaying 10% of less wear compared to MoM type artificial hip implant. The application of thinner acetabular cup is possible using CoC type due its strength. Thus, larger femoral head can be fitted into smaller acetabular shell. Besides that, it offers



wider motion range, good bearing and higher stability in young patients. However, CoC artificial hip implants are expensive, squeaking, brittle and unpleasant to patients (Wu *et al.*, 2016).

**MoM:** The key advantage of MoM type artificial hip implant is hardness differences. The MoM type artificial hip implants are manufactured from various metallic alloys i.e. cobalt-chromium alloys. MoM type implants are hard and not brittle compared to ceramic types. Meanwhile, MoM hip implants displaying higher scratch and wear resistance when compared with plastic type. MoM type also permits larger femoral head diameter for constant acetabular shell size which able to provide wider hip motion range along with lower bone resorption, less wear, lower dislocation risk, minimised offset problems and easier revision surgery. The MoM coupling is susceptible to metallosis and infection which leads to increased failure rate (Milošev *et al.*, 2000). Thus, there is great necessity for smooth articulating bearing surface in femoral head and acetabular cup to minimise wear accompanied by allowing required hip movement. It has been suggested that UHMWPE acetabular cup with cobalt-chrome femoral head offer excellent bearing surfaces combination. Besides that, the combination of cobalt-chrome femoral head and titanium modular stem extensively used in hip related orthopaedic devices (English *et al.*, 2015).

## 2.7 Metallic artificial femoral stem

The artificial femoral stem design transformed in many ways in term of design since the introduction of Charnley femoral stem in 1960's. As a result, more diverse types of artificial stems are manufactured as shown in Figure 2.6. Artificial hip implant technology continuously evolving as new methodologies and designs have been introduced. There are 62 types of artificial hip implant manufactured by 19 different companies (Hongyu & Blunt, 2009).





Figure 2.6: Different artificial femoral stem designs (Hongyu & Blunt, 2009)

The metallic artificial femoral stem offers geometry and cost flexibilities without any doubt. However, difficulty arises in choosing optimal artificial femoral stem for patients by considering long term follow up requirement in order to evaluate new femoral stem performance (Salentiny *et al.*, 2018). It is reported that several new designs cause patient's discomfort and premature failure which requires revision surgery in less than 5 years. Thus, new femoral should be tested in term of sustainability before market release. Continuous development should be given an insight to improve longevity of total hip replacement surgery (THR) (Johanson, 2017). In recent time, Charnley, Stanmore, Exeter and Müller artificial femoral stems are used as benchmark compared to other stem designs due to better evaluation and long term durability (Hongyu & Blunt, 2009).

There are two major design categories such as modular and monoblock artificial femoral stems as shown in Figure 2.7. Femoral stem and head are fabricated as a single component in modular stem design which able to solve complications of monoblock design femoral stem application in special hip joint anatomy patients (Hongyu & Blunt, 2009). In addition, modular design femoral stem provides flexibility of femoral head size, neck length and combination material variation. For example, combination of material improves the wear resistance in femoral head (cobalt chrome alloy) and excellent mechanical properties is achieved by femoral stems when

manufactured by titanium alloys or stainless steel. Femoral head polished smoothly prior to fixation with femoral stem to facilitate less friction rotation in prosthetic socket.

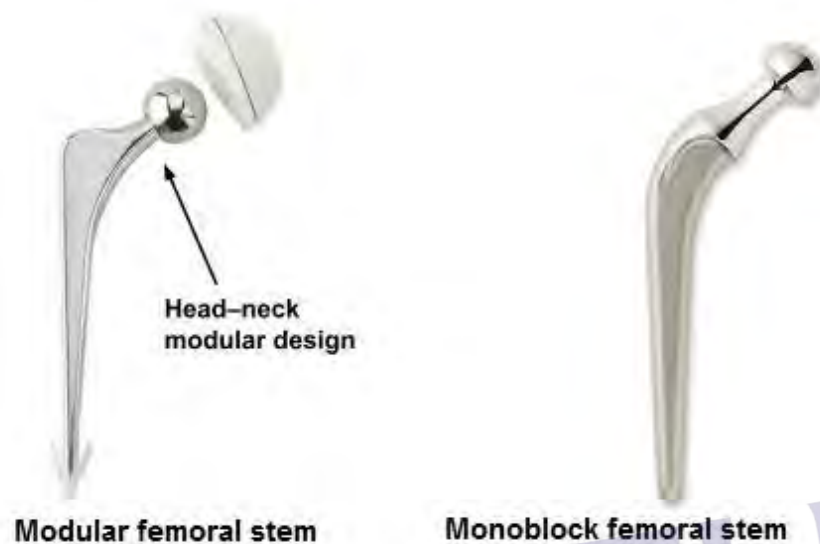


Figure 2.7: Different designs of artificial femoral stems (Hongyu & Blunt, 2009)

### 2.7.1 Stem material

In artificial femoral stem designing process many variables such as material, geometry and surface finish should be considered. Optimal tribological and mechanical characteristics, biocompatibility, human body physical environment and loading regime in femoral stem significantly influences material selection (Hongyu & Blunt, 2009).

The material of artificial femoral stem should withstand active individual's physical loading according to their activities and day-to-day utilisation. The material's strength in term of yielding and fatigue no longer a critical issue as most of the materials used to fabricate femoral stems are stronger. However, stress shielding should be given an attention as one of the material selection design constraint. Reduction in bone density as stiffer implant transmits much load and initiating high

stress gradient between femur lower section and cancellous bone is known as stress shielding (Hongyu & Blunt, 2009).

Stress shielding can cause discomfort and pain to patients. Therefore, material selection should be performed considering similar stiffness, strength, mechanical properties and density to minimise stress shielding effect. Lately, titanium alloys, cobalt chrome alloys and stainless steels are most common materials to manufacture artificial femoral stem because of their excellent biocompatibility, tribological and mechanical characteristics (Nagentrau *et al.*, 2019).

Unfortunately, these materials are much stiffer with higher yield strength than bone which might results in stress shielding. Besides that, artificial femoral stem made from titanium alloys susceptible to fail earlier compared to cobalt chromium and stainless-steel materials as occurrence of crevice corrosion due to gap generation between stem-bone/cement or head-taper. Present study focussing on artificial hip stem manufactured from titanium alloy.

### 2.7.2 Stem geometry

Stem geometry is an important variable in artificial femoral design as it can affect directly in-vivo behaviour and subsequent failure mechanism of total hip replacement (THR) (Fokter *et al.*, 2017). In fact, certain artificial femoral stems have been removed from market due to their poor short-term survival rate which is highly design dependent. The optimal design of femoral stem should be able to transfer load in axial and torsional direction without stress singularity and excessive micromotion between cement-implant (cemented THR) and HAp-implant (uncemented THR) interfaces as shown in Figure 2.8.

Artificial femoral stem geometry encompasses overall shape (anatomical/symmetrical), cross-section (square/oval), flange and collar presence, stem tip shape and stem length. Besides that, double/triple taper design and greater/lesser degree of rounded edges are influencing stem geometry (Hongyu & Blunt, 2009). Femoral stems with symmetrical geometry design exhibiting excellent clinical performance. The number of artificial femoral hip stem geometry designs rapidly increasing in market. Thus, effective clinical assessment in term of performance and durability should be performed on new design femoral stem.

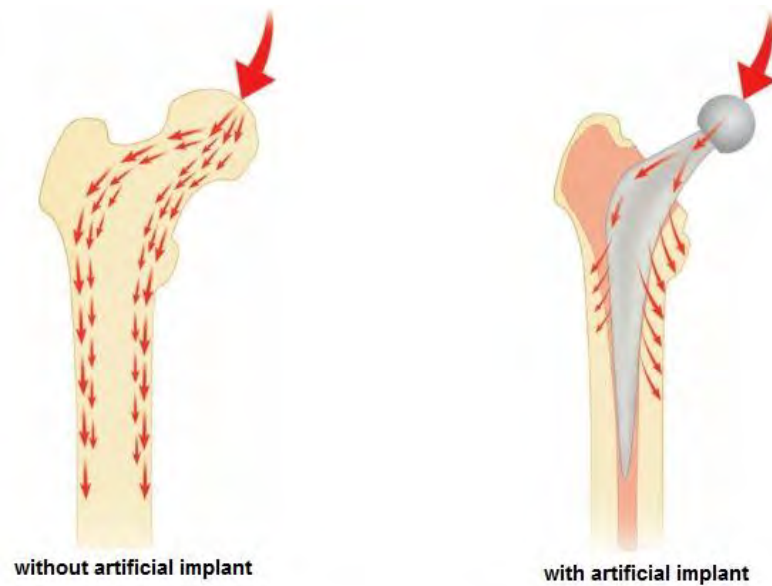


Figure 2.8: Load transfer pattern with and without artificial hip implant (Hongyu & Blunt, 2009)

### 2.7.3 Stem surface finish

Artificial femoral stem surface finish is another vital design property which varies among different types of femoral stems. The effect of stem surface finish on total hip replacement (THR) performance has been disputed for a long time as no specific standard is available regarding this variable (Hongyu & Blunt, 2009). Certainly, the texture of the femoral stem surface has a direct influence on bonding strength at stem-HAp coating/stem-cement interfaces. Matte femoral stems could promote bond strength at the interface compared to polished femoral stems, as HAp coating or bone cement attachment will be enhanced.

Matte and polished femoral stems are often known as closed design and force-closed design, which depend on stem mechanical taper locking to accomplish self-tightening properties. Although a matte surface finished stem can promote bonding at the interface but is inclined to generate more debris and sourcing severe interfacial damage once delamination/debonding occurs. This indicates that thick and good quality interfaces with strong bonding are required to minimize delamination failure. From a clinical point of view, stem surface finish is a complex matter and still under investigation since there is not



## REFERENCES

- Abd-elsayed, A. (2019). *Pain: A Review Guide*. Madison, WI USA: Springer.
- Abdelgaied, A., Liu, F., Brockett, C., Jennings, L., Fisher, J., & Jin, Z. (2011). Computational wear prediction of artificial knee joints based on a new wear law and formulation. *Journal of Biomechanics*, 44(6), 1108–1116.
- Apostu, D., Lucaciu, O., Berce, C., Lucaciu, D., & Cosma, D. (2018). Current methods of preventing aseptic loosening and improving osseointegration of titanium implants in cementless total hip arthroplasty: a review. *Journal of International Medical Research*, 46(6), 2104–2119.
- Archard, J. F. (1953). Contact and rubbing of flat surfaces. *Journal of Applied Physics*, 24(8), 981–988.
- Arslan, O., & Dag, S. (2018). Contact mechanics problem between an orthotropic graded coating and a rigid punch of an arbitrary profile. *International Journal of Mechanical Sciences*, 135, 541–554.
- Ashkanfar, A., Langton, D. J., & Joyce, T. J. (2017). Does a micro-grooved trunnion stem surface finish improve fixation and reduce fretting wear at the taper junction of total hip replacements? A finite element evaluation. *Journal of Biomechanics*, 63, 47–54.
- Balci, M. N., & Dag, S. (2020). Moving contact problems involving a rigid punch and a functionally graded coating. *Applied Mathematical Modelling*, 81, 855–886.
- Bitter, T., Khan, I., Marriott, T., Lovelady, E., Verdonschot, N., & Janssen, D. (2018). Finite element wear prediction using adaptive meshing at the modular taper interface of hip implants. *Journal of the Mechanical Behavior of Biomedical Materials*, 77, 616–623.
- Boye, P. (2019). The use of multiple linear regressions in determining the relationship between housing unit price and some major components in a real estate building. *Scottish Journal of Arts, Social Sciences and Scientific Studies*, April, 3–17.
- Braunovic, M. (2009). Fretting in electrical/electronic connections: a review. *IEICE*



PTTA UTM  
 PERPUSTAKAAN TUNJUNG AMINAH

*Transactions on Electronics, E92-C(8)*, 982–991.

- Brown, S. A., & Lemons, J. E. (1996). Medical applications of titanium and its alloys: the material and biological issues. *Medical Applications of Titanium and Its Alloys: The Material and Biological Issues*. West Conshohocken, PA: ASTM.
- Catalina, T., Iordache, V., & Caracaleanu, B. (2013). Multiple regression model for fast prediction of the heating energy demand. *Energy & Buildings*, *57*, 302–312.
- Chai, H. (2003). Fracture mechanics analysis of thin coatings under spherical indentation. *International Journal of Fracture*, *119(3)*, 263–285.
- Chen, J. J., Liu, L., Li, S. X., Yu, S. R., & He, Y. N. (2018). Experimental and numerical investigation on crack initiation of fretting fatigue of dovetail. *Fatigue and Fracture of Engineering Materials and Structures*, *41(6)*, 1426–1436.
- Çömez, İ., Yılmaz, K., Güler, M., & Yıldırım, B. (2019). Frictionless contact problem between a rigid moving punch and a homogeneous layer resting on a Winkler foundation. *Journal of Structural Engineering & Applied Mechanics*, *2(2)*, 75–87.
- Cornec, A., Scheider, I., & Schwalbe, K. H. (2003). On the practical application of the cohesive model. *Engineering Fracture Mechanics*, *70(14)*, 1963–1987.
- Dey, A., Mukhopadhyay, A. K., Gangadharan, S., Sinha, M. K., & Basu, D. (2009). Characterization of microplasma sprayed hydroxyapatite coating. *Journal of Thermal Spray Technology*, *18(4)*, 578–592.
- Di Leo, C. V., Luk-Cyr, J., Liu, H., Loeffel, K., Al-Athel, K., & Anand, L. (2014). A new methodology for characterizing traction-separation relations for interfacial delamination of thermal barrier coatings. *Acta Materialia*, *71*, 306–318.
- Ding, J., Leen, S. B., & McColl, I. R. (2004). The effect of slip regime on fretting wear-induced stress evolution. *International Journal of Fatigue*, *26(5)*, 521–531.
- dos Santos, C. T., Barbosa, C., Monteiro, M. J., Abud, I. C., Caminha, I. M. V., & Roesler, C. R. M. (2016). Characterization of the fretting corrosion behavior, surface and debris from head-taper interface of two different modular hip prostheses. *Journal of the Mechanical Behavior of Biomedical Materials*, *62*, 71–82.
- Elkins, J. M., Callaghan, J. J., & Brown, T. D. (2014). Stability and trunnion wear potential in large-diameter metal-on-metal total hips: A finite element analysis. *Clinical Orthopaedics and Related Research*, *472(2)*, 529–542.
- Elkins, J. M., O'Brien, M. K., Stroud, N. J., Pedersen, D. R., Callaghan, J. J., & Brown,



- T. D. (2011). Hard-on-hard total hip impingement causes extreme contact stress concentrations. *Clinical Orthopaedics and Related Research*, 469(2), 454–463.
- English, R., Ashkanfar, A., & Rothwell, G. (2015). A computational approach to fretting wear prediction at the head-stem taper junction of total hip replacements. *Wear*, 338–339, 210–220.
- English, R., Ashkanfar, A., & Rothwell, G. (2016). The effect of different assembly loads on taper junction fretting wear in total hip replacements. *Tribology International*, 95, 199–210.
- Eschweiler, J., Fieten, L., Dell'Anna, J., Kabir, K., Gravius, S., Tingart, M., & Radermacher, K. (2012). Application and evaluation of biomechanical models and scores for the planning of total hip arthroplasty. *Proceedings of the Institution of Mechanical Engineers, Part H: Journal of Engineering in Medicine*, 226(12), 955–967.
- Fallahnezhad, K. (2018). *An Investigation on the Fretting Wear and Corrosion Damage to the Head Neck Interface of Total Hip Replacement : A Finite Element Modelling Approach*. Flinders University: Ph.D. Thesis.
- Fallahnezhad, K., Oskouei, R. H., Badnava, H., & Taylor, M. (2017). An adaptive finite element simulation of fretting wear damage at the head-neck taper junction of total hip replacement: The role of taper angle mismatch. *Journal of the Mechanical Behavior of Biomedical Materials*, 75, 58–67.
- Fallahnezhad, K., Oskouei, R. H., Badnava, H., & Taylor, M. (2019). The influence of assembly force on the material loss at the metallic head-neck junction of hip implants subjected to cyclic fretting wear. *Metals*, 9(4), 422.
- Farmand-Ashtiani, E., Alanis, D., Cugnoni, J., & Botsis, J. (2015). Delamination in cross-ply laminates: Identification of traction-separation relations and cohesive zone modeling. *Composites Science and Technology*, 119, 85–92.
- Fialho, J. C., Fernandes, P. R., Eça, L., & Folgado, J. (2007). Computational hip joint simulator for wear and heat generation. *Journal of Biomechanics*, 40(11), 2358–2366.
- Fokter, S. K., Moličnik, A., Kavalarič, R., Pelicon, P., Rudolf, R., & Gubelj, N. (2017). Why do some titanium-alloy total hip arthroplasty modular necks fail? *Journal of the Mechanical Behavior of Biomedical Materials*, 69, 107–114.
- Fouvry, S., Kapsa, P., & Vincent, L. (2001). Elastic-plastic shakedown analysis of fretting wear. *Wear*, 247(1), 41–54.



- Graves, S. E., Davidson, D., Ingerson, L., Ryan, P., Griffith, E. C., McDermott, B. F. J., McElroy, H. J., & Pratt, N. L. (2004). The Australian Orthopaedic Association National Joint Replacement Registry. *Medical Journal of Australia*, 180(5), S31-S34.
- Guipont, V., Jeandin, M., Bansard, S., Khor, K. A., Nivard, M., Berthe, L., Cuq-Lelandais, J. P., & Boustie, M. (2010). Bond strength determination of hydroxyapatite coatings on Ti-6Al-4V substrates using the LAser Shock Adhesion Test (LASAT). *Journal of Biomedical Materials Research - Part A*, 95(4), 1096–1104.
- Haibo Wang, B. S. (2004). *Hydroxyapatite Degradation and Biocompatibility*. The Ohio State University: Ph.D. Thesis.
- Hasan, M. F., Wang, J., & Berndt, C. (2014). Evaluation of the mechanical properties of plasma sprayed hydroxyapatite coatings. *Applied Surface Science*, 303, 155–162.
- Hermes, F. H. (2010). *Process Zone and Cohesive Element Size in Numerical Simulations of Delamination in Bi-Layers*. Eindhoven University of Technology: Ph.D. Thesis.
- Hibbeler, R. C. (2013). *Statics and mechanics of materials*. Pearson Higher Ed.
- Hills, D. A., Nowell, D., & Barber, J. R. (2017). KL Johnson and contact mechanics. *Proceedings of the Institution of Mechanical Engineers, Part C: Journal of Mechanical Engineering Science*, 231(13), 2451–2458.
- Hongyu, Z., & Blunt, P. L. (2009). *The Influence of Stem Design and Fixation Methods on the Lifetime of Total Hip Replacement*. University of Huddersfield: Ph.D. Thesis.
- Jang, J., Sung, M., Han, S., & Yu, W. R. (2017). Prediction of delamination of steel-polymer composites using cohesive zone model and peeling tests. *Composite Structures*, 160, 118–127.
- Jimenez, S., & Duddu, R. (2016). On the parametric sensitivity of cohesive zone models for high-cycle fatigue delamination of composites. *International Journal of Solids and Structures*, 82, 111–124.
- Jin, O., & Mall, S. (2004). Effects of slip on fretting behavior: Experiments and analyses. *Wear*, 256(7–8), 671–684.
- Johanson, P. (2017). *Improvements in Hip Arthroplasty - Did They Work ? Evaluation of Different Articulations and Fixation Concepts*. University of Gothenburg:



PTTA UTHM  
PEPUSIAKAM TUKUTUKAMINAH

Ph.D. Thesis.

- Kohn, D. H. (1998). Metals in medical applications. *Current Opinion in Solid State and Materials Science*, 3(3), 309–316.
- Laonapakul, T., Otsuka, Y., & Mutoh, Y. (2011). Fatigue and acoustic emission behavior of plasma sprayed HAp top coat and HAp/Ti bond coat with HAp top coat on commercially pure titanium. *Key Engineering Materials*, 452–453, 857–860.
- Laonapakul, T., Rakngarm Nimkerdphol, A., Otsuka, Y., & Mutoh, Y. (2012). Failure behavior of plasma-sprayed HAp coating on commercially pure titanium substrate in simulated body fluid (SBF) under bending load. *Journal of the Mechanical Behavior of Biomedical Materials*, 15, 153–166.
- Li, J., & Lu, Y. H. (2013). Effects of displacement amplitude on fretting wear behaviors and mechanism of Inconel 600 alloy. *Wear*, 304(1–2), 223–230.
- Lindahl, C. (2012). *Biomimetic Deposition of Hydroxyapatite on Titanium Implant Material*. Uppsala University: Ph.D. Thesis.
- Liu, F., Leslie, I., Williams, S., Fisher, J., & Jin, Z. (2008). Development of computational wear simulation of metal-on-metal hip resurfacing replacements. *Journal of Biomechanics*, 41(3), 686–694.
- Loeser, R. F. (2006). Molecular mechanisms of cartilage destruction: Mechanics, inflammatory mediators, and aging collide. *Arthritis and Rheumatism*, 54(5), 1357–1360.
- Lu, P., & Chou, K. (2013). Interface delamination of diamond-coated carbide tools considering coating fractures by XFEM. *ASME 2013 International Manufacturing Science and Engineering Conference Collocated with the 41st North American Manufacturing Research Conference, MSEC 2013*, 1, 1–9.
- Lu, X., Ridha, M., Chen, B. Y., Tan, V. B. C., & Tay, T. E. (2019). On cohesive element parameters and delamination modelling. *Engineering Fracture Mechanics*, 206(August 2018), 278–296.
- Madge, J. J., Leen, S. B., McColl, I. R., & Shipway, P. H. (2007). Contact-evolution based prediction of fretting fatigue life: Effect of slip amplitude. *Wear*, 262(9–10), 1159–1170.
- Madge, J. J., Leen, S. B., & Shipway, P. H. (2007). The critical role of fretting wear in the analysis of fretting fatigue. *Wear*, 263, 542–551.
- Madge, J. J., Leen, S. B., & Shipway, P. H. (2008). A combined wear and crack





- nucleation-propagation methodology for fretting fatigue prediction. *International Journal of Fatigue*, 30(9), 1509–1528.
- Malahias, M. A., Kostretzis, L., Greenberg, A., Nikolaou, V. S., Atrey, A., & Sculco, P. K. (2020). Highly Porous Titanium Acetabular Components in Primary and Revision Total Hip Arthroplasty: A Systematic Review. *Journal of Arthroplasty*, 35(6), 1737-1749.
- Maslan, M. H. (2015). *Development of Predictive Finite Element Models for Complete Contact Fretting Fatigue*. University of Manchester: Ph.D. Thesis.
- Matveevsky, R. M. (1965). The critical temperature of oil with point and line contact machines. *Journal of Fluids Engineering, Transactions of the ASME*, 87(3), 754–759.
- McColl, I. R., Ding, J., & Leen, S. B. (2004). Finite element simulation and experimental validation of fretting wear. *Wear*, 256(11–12), 1114–1127.
- McManamon, C., De Silva, J. P., Power, J., Ramirez-Garcia, S., Morris, M. A., & Cross, G. L. W. (2014). Interfacial Characteristics and Determination of Cohesive and Adhesive Strength of Plasma-Coated Hydroxyapatite Via Nanoindentation and Microscratch Techniques. *Langmuir*, 30(38), 11412–11420.
- Milošev, L., Antolič, V., Minovič, A., Cör, A., Herman, S., Pavlovčič, V., & Campbell, P. (2000). Extensive metallosis and necrosis in failed prostheses with cemented titanium-alloy stems and ceramic heads. *Journal of Bone and Joint Surgery - Series B*, 82(3), 352–357.
- Mohd Tobi, A. L., Ding, J., Bandak, G., Leen, S. B., & Shipway, P. H. (2009). A study on the interaction between fretting wear and cyclic plasticity for Ti-6Al-4V. *Wear*, 267(1–4), 270–282.
- Mohd Tobi, A. L., Ding, J., Pearson, S., Leen, S. B., & Shipway, P. H. (2010). The effect of gross sliding fretting wear on stress distributions in thin W-DLC coating systems. *Tribology International*, 43(10), 1917–1932.
- Mohd Tobi, A. L., Shipway, P. H., & Leen, S. B. (2013). Finite element modelling of brittle fracture of thick coatings under normal and tangential loading. *Tribology International*, 58, 29–39.
- Morris, J. E. (2006). Nanopackaging: Nanotechnologies and Electronics Packaging. *Electronics System integration Technology Conference*, 1–44. Springer, Cham.
- Nagentrau, M., Mohd Tobi, A. L., Jamian, S., & Otsuka, Y. (2019). Contact slip prediction in HA<sub>p</sub> coated artificial hip implant using finite element analysis.



*Mechanical Engineering Journal*, 6(3), 18-00562-18–00562.

- Nagentrau, M., Siswanto, W. A., & Mohd Tobi, A. L. (2016). Predicting the sliding amplitude of plastic deformation in the reciprocating sliding contact. *ARPN Journal of Engineering and Applied Sciences*, 11(4), 2266–2271.
- Nagentrau, M., Siswanto, W. A., & Mohd Tobi, A. L. (2015). Investigation on the effect of linear kinematic hardening model on plasticity prediction of reciprocating sliding contact. *Applied Mechanics and Materials*, 773–774, 183–187.
- Nagentrau, M., Mohd Tobi, A. L., Jamian, S., & Otsuka, Y. (2020). HAp coated hip prosthesis contact pressure prediction using FEM analysis. *Materials Science Forum*, 991, 53–61.
- Nyman, J. S., Leng, H., Neil Dong, X., & Wang, X. (2009). Differences in the mechanical behavior of cortical bone between compression and tension when subjected to progressive loading. *Journal of the Mechanical Behavior of Biomedical Materials*, 2(6), 613–619.
- Otsuka, Y., Kawaguchi, H., & Mutoh, Y. (2016). Cyclic delamination behavior of plasma-sprayed hydroxyapatite coating on Ti-6Al-4V substrates in simulated body fluid. *Materials Science and Engineering C*, 67, 533–541.
- Otsuka, Y., Kojima, D., & Mutoh, Y. (2016). Prediction of cyclic delamination lives of plasma-sprayed hydroxyapatite coating on Ti-6Al-4V substrates with considering wear and dissolutions. *Journal of the Mechanical Behavior of Biomedical Materials*, 64, 113–124.
- Otsuka, Y., Miyashita, Y., & Mutoh, Y. (2016). Effects of delamination on fretting wear behaviors of plasma-sprayed hydroxyapatite coating. *Mechanical Engineering Journal*, 3(2), 15-00573-15–00573.
- Ovcharenko, A., & Etsion, I. (2009). Junction growth and energy dissipation at the very early stage of elastic-plastic spherical contact fretting. *Journal of Tribology*, 131(3), 1–8.
- Peng, B., Akil, H.R., & Khan, A. (2015). Tribology International Optimization on wear performance of UHMWPE composites using response surface methodology. *Tribology International*, 88, 252–262.
- Peng, L., Gong, X., Wong, K., & Guillaumat, L. (2012). Application of cohesive-zone models to delamination behaviour of composite material. *World Journal of Engineering*, 9(2), 109–118.



- Petroutsatou, C., Lambropoulos, S., & Pantouvakis, J. (2006). Road tunnel early cost estimates using multiple regression analysis. *Operational Research: An International Journal*, 6(3), 311–322.
- Reddy, J. N. (2017). *Energy Principles and Variational Methods in Applied Mechanics*. John Wiley & Sons.
- Ren, F., Case, E. D., Morrison, A., Tafesse, M., & Baumann, M. J. (2009). Resonant ultrasound spectroscopy measurement of Young's modulus, shear modulus and Poisson's ratio as a function of porosity for alumina and hydroxyapatite. *Philosophical Magazine*, 89(14), 1163–1182.
- Sakai, R., Takahashi, A., Takahira, N., Uchiyama, K., Yamamoto, T., Uchida, K., Fukushima, K., Moriya, M., Takaso, M., Itoman, M., & Mabuchi, K. (2011). Hammering force during cementless total hip arthroplasty and risk of microfracture. *HIP International*, 21(3), 330–335.
- Salentiny, Y., Zwicky, L., Ochsner, P. E., & Clauss, M. (2018). Long-term survival of the cemented Müller CDH stem: a minimum follow-up of 10 years. *Archives of Orthopaedic and Trauma Surgery*, 138(10), 1471–1477.
- Sauger, E., Fouvry, S., Ponsonnet, L., Kapsa, P., Martin, J. M., & Vincent, L. (2000). Tribologically transformed structure in fretting. *Wear*, 245(1–2), 39–52.
- Shen, S., Lee, H. P., Lim, S. P., & Ong, C. J. (2014). Three-dimensional finite element analysis of interfacial delamination in traveling wave ultrasonic motors. *International Journal of Damage Mechanics*, 23(7), 964–978.
- Shi, L., Wei, D. S., Wang, Y. R., Tian, A. M., & Li, D. (2016). An investigation of fretting fatigue in a circular arc dovetail assembly. *International Journal of Fatigue*, 82, 226–237.
- Siswanto, W. A., Nagentrau, M., Mohd Tobi, A. L., & Tamin, M. N. (2016). Prediction of plastic deformation under contact condition by quasi-static and dynamic simulations using explicit finite element analysis. *Journal of Mechanical Science and Technology*, 30(11), 5093–5101.
- Siswanto, W. A., Nagentrau, M., Mohd Tobi, A. L., & Tamin, M. N. (2015). Contact pressure prediction comparison using implicit and explicit finite element methods and the validation with Hertzian theory. *International Journal of Mechanical and Mechatronics Engineering*, 15(6), 1–8.
- Soutis, C., & Kashtalyan, M. (2003). Strain energy release rate for crack tip delaminations in angle-ply continuous fibre reinforced composite laminates. In





*European Structural Integrity Society*, 32, 455-463. Elsevier.

- Souza, R. M., Sinatora, A., Mustoe, G. G. W., & Moore, J. J. (2001). Numerical and experimental study of the circular cracks observed at the contact edges of the indentations of coated systems with soft substrates. *Wear*, 250(251), 1337–1346.
- Surajit, P., & Susanta Kumar, G. (2010). Multi-response optimization using multiple regression-based weighted signal-to-noise ratio (MRWSN). *Quality Engineering*, June 2013, 37–41.
- System, A. K. (2019). *Australian Orthopaedic Association National Joint Replacement Registry : Automated Industry Reporting System*. Adelaide.
- Turon, A., Camanho, P. P., Costa, J., & Renart, J. (2010). Accurate simulation of delamination growth under mixed-mode loading using cohesive elements: Definition of interlaminar strengths and elastic stiffness. *Composite Structures*, 92(8), 1857–1864.
- Turon, A., Dávila, C. G., Camanho, P. P., & Costa, J. (2007). An engineering solution for mesh size effects in the simulation of delamination using cohesive zone models. *Engineering Fracture Mechanics*, 74(10), 1665–1682.
- Uddin, M. S., & Zhang, L. C. (2013). Predicting the wear of hard-on-hard hip joint prostheses. *Wear*, 301(1–2), 192–200.
- Vadiraj, A., & Kamaraj, M. (2006). Characterization of fretting fatigue damage of PVD TiN coated biomedical titanium alloys. *Surface and Coatings Technology*, 200(14–15), 4538–4542.
- van Hal, B. A. E., Peerlings, R. H. J., Geers, M. G. D., & van der Sluis, O. (2007). Cohesive zone modeling for structural integrity analysis of IC interconnects. *Microelectronics Reliability*, 47(8), 1251–1261.
- Verdonschot, N. (2005). Implant Choice: Stem Design Philosophies. *The Well-Cemented Total Hip Arthroplasty*, 168–179. Springer, Berlin, Heidelberg.
- Vingsbo, O., & Söderberg, S. (1988). On fretting maps. *Wear*, 126(2), 131–147.
- Wang, S., Wang, F., Liao, Z., Wang, Q., Liu, Y., & Liu, W. (2015). Study on torsional fretting wear behavior of a ball-on-socket contact configuration simulating an artificial cervical disk. *Materials Science and Engineering C*, 55, 22–33.
- Wong, K. J., Gong, X. J., Aivazzadeh, S., & Tamin, M. N. (2012). Numerical simulation of mode I delamination behaviour of multidirectional composite laminates with fibre bridging effect. *ECCM 2012 - Composites at Venice, Proceedings of the 15th European Conference on Composite Materials, June*,



24–28.

- Wu, G. L., Zhu, W., Zhao, Y., Ma, Q., & Weng, X. S. (2016). Hip squeaking after ceramic-on-ceramic total hip arthroplasty. *Chinese Medical Journal*, 129(15), 1861–1866.
- Yang, C. W., & Lui, T. S. (2007). Effect of crystallization on the bonding strength and failures of plasma-sprayed hydroxyapatite. *Materials Transactions*, 48(2), 211–218.
- Yang, Q., Zhou, W., Gai, P., Zhang, X., Fu, X., Chen, G., & Li, Z. (2017). Investigation on the fretting fatigue behaviors of Ti-6Al-4V dovetail joint specimens treated with shot-peening. *Wear*, 372–373, 81–90.
- Yang, Y. C., Chang, E., & Lee, S. Y. (2003). Mechanical properties and Young's modulus of plasma-sprayed hydroxyapatite coating on Ti substrate in simulated body fluid. *Journal of Biomedical Materials Research - Part A*, 67(3), 886–899.
- Yoshimoto, K., Nakashima, Y., Nakamura, A., Mawatari, T., Todo, M., Hara, D., & Iwamoto, Y. (2015). Neck fracture of femoral stems with a sharp slot at the neck: biomechanical analysis. *Journal of Orthopaedic Science*, 20(5), 881–887.
- Yue, T. (2017). *Finite Element Analysis of Fretting Wear*. Ghent University: Ph.D. Thesis..
- Yue, T., & Wahab, M. A. (2019). A review on fretting wear mechanisms, models and numerical analyses. *Computers, Materials and Continua*, 59(2), 405–432.
- Yugeswaran, S., Yoganand, C. P., Kobayashi, A., Paraskevopoulos, K. M., & Subramanian, B. (2012). Mechanical properties, electrochemical corrosion and in-vitro bioactivity of yttria stabilized zirconia reinforced hydroxyapatite coatings prepared by gas tunnel type plasma spraying. *Journal of the Mechanical Behavior of Biomedical Materials*, 9, 22–33.
- Zhang, H. Y., Blunt, L., Jiang, X. Q., Brown, L., Barrans, S., & Zhao, Y. (2008). Femoral stem wear in cemented total hip replacement. *Proceedings of the Institution of Mechanical Engineers, Part H: Journal of Engineering in Medicine*, 222(5), 583–592.
- Zhang, L., Ge, S., Liu, H., Wang, Q., Wang, L., & Xian, C. J. (2015). Contact damage failure analyses of fretting wear behavior of the metal stem titanium alloy-bone cement interface. *Journal of the Mechanical Behavior of Biomedical Materials*, 51, 132–146.
- Zhang, T., Harrison, N. M., McDonnell, P. F., McHugh, P. E., & Leen, S. B. (2013).



PT TUN AMINAH  
REPUSTAKAN TOKIL TUN AMINAH

A finite element methodology for wear-fatigue analysis for modular hip implants. *Tribology International*, 65, 113–127.

Zhang, T., McHugh, P. E., & Leen, S. B. (2011). Computational study on the effect of contact geometry on fretting behaviour. *Wear*, 271(9–10), 1462–1480.

Zhou, Q. C., Ju, Y. T., Wei, Z., Han, B., & Zhou, C. S. (2014). Cohesive zone modeling of propellant and insulation interface debonding. *Journal of Adhesion*, 90(3), 230–251.

Zhu, M. H., & Zhou, Z. R. (2011). On the mechanisms of various fretting wear modes. *Tribology International*, 44(11), 1378–1388.

Zhu, W., Yang, L., Guo, J. W., Zhou, Y. C., & Lu, C. (2014). Numerical study on interaction of surface cracking and interfacial delamination in thermal barrier coatings under tension. *Applied Surface Science*, 315(1), 292–298.

Zhu, W., Yang, L., Guo, J. W., Zhou, Y. C., & Lu, C. (2015). Determination of interfacial adhesion energies of thermal barrier coatings by compression test combined with a cohesive zone finite element model. *International Journal of Plasticity*, 64, 76–87.



PTTA UTHM  
PERPUSTAKAAN TUNKU TUN AMINAH